AD-A152 292

**BRL**

MEMORANDUM REPORT BRL-MR-3418

AD

⑫

# NUMERICAL RESOLUTION CALCULATION FOR ELASTIC-PLASTIC IMPACT PROBLEMS

Bertina M. Creighton

December 1984

DTIC
ELECTE
MAR 2 7 1985
S
B
D

**US ARMY BALLISTIC RESEARCH LABORATORY**
**ABERDEEN PROVING GROUND, MARYLAND**

85  3  27  050

| REPORT DOCUMENTATION PAGE | | READ INSTRUCTIONS BEFORE COMPLETING FORM |
|---|---|---|
| 1 REPORT NUMBER<br><br>MEMORANDUM REPORT   BRL-MR-3418 | 2. GOVT ACCESSION NO.<br><br>AD-A152-292 | 3. RECIPIENT'S CATALOG NUMBER |
| 4. TITLE (and Subtitle)<br><br>NUMERICAL RESOLUTION CALCULATION FOR ELASTIC-PLASTIC IMPACT PROBLEMS | | 5. TYPE OF REPORT & PERIOD COVERED<br><br>FINAL |
| | | 6. PERFORMING ORG. REPORT NUMBER |
| 7. AUTHOR(s)<br><br>Bertina M. Creighton | | 8. CONTRACT OR GRANT NUMBER(s) |
| 9. PERFORMING ORGANIZATION NAME AND ADDRESS<br>US Army Ballistic Research Laboratory<br>ATTN: AMXBR-TBD<br>Aberdeen Proving Ground, MD  21005-5066 | | 10. PROGRAM ELEMENT, PROJECT, TASK AREA & WORK UNIT NUMBERS<br><br>1L162618AH80 |
| 11. CONTROLLING OFFICE NAME AND ADDRESS<br>US Army Ballistic Research Laboratory<br>ATTN: AMXBR-OD-ST<br>Aberdeen Proving Ground, MD  21005-5066 | | 12. REPORT DATE<br><br>December 1984 |
| | | 13. NUMBER OF PAGES<br><br>76 |
| 14 MONITORING AGENCY NAME & ADDRESS(If different from Controlling Office) | | 15. SECURITY CLASS. (of this report)<br><br>UNCLASSIFIED |
| | | 15a. DECLASSIFICATION/DOWNGRADING SCHEDULE |

16 DISTRIBUTION STATEMENT (of this Report)

Approved for public release; distribution unlimited.

17. DISTRIBUTION STATEMENT (of the abstract entered in Block 20, if different from Report)

18. SUPPLEMENTARY NOTES

19. KEY WORDS (Continue on reverse side if necessary and identify by block number)

Wave Propagation
Elastic-plastic Impact
Mesh Orientation
Skalak's Approximation
One-dimensional Wave Equation

Airy's Integral
Artificial Viscosity

20 ABSTRACT (Continue on reverse side if necessary and identify by block number)

This paper is a brief summary of an investigation using the finite element method in the study of wave propagation and impact problems in solid materials. Guidelines are provided for the determination of the computational grid and the shape and size of the elements. Two examples are presented to show effects of mesh refinements on solution accuracy. Problems concerning the effects of artificial viscosity, as well as pressure and strain changes in the orientation of the grid, are presented. This study was performed with EPIC-2, a computer code for

DD FORM 1473 EDITION OF 1 NOV 65 IS OBSOLETE

elastic-plastic impact calculations in two dimensions. EPIC-2 makes use of triangular elements in several configurations. The results presented herein should serve as a quide to proper selection of mesh size and orientation for accurate representation of physical problems.

# TABLE OF CONTENTS

DTIC
ELECTE
MAR 2 7 1985
S          D
B

Accession For

NTIS GRA&I
DTIC TAB
Unannounced
Justification

By
Distribution/
Availability Codes
Avail and/or
Dist     Special

A-1

3

## LIST OF ILLUSTRATIONS

# I. INTRODUCTION

The finite element method has been used in the modeling of many problems concerning elastic-plastic impact behavior. The correct geometric representation of a mesh is important in obtaining accurate results without introducing numerical instabilities into the calculations. Here, triangular elements formulated for wave propagation and shock problems have been applied to both a classical elastic wave propagation problem and to the analysis of a system subjected to high velocity impact loading.

The objective of this study is to ascertain the effects of different orientations of the triangular elements and to determine the optimal mesh size and shape using EPIC-2, a computer code for elastic-plastic impact calculations in two dimensions, to best fit the solution. The information presented here is intended to be of assistance to potential users faced with applying the finite element method to impact problems and considering how to obtain meaningful solutions in two dimensions.

Wave propagation in the impact of a semi-infinite elastic bar was chosen because of the availability of a closed form solution. The analytical solution obtained by Richard Skalak,[1] and the elementary one-dimensional theory for elastic wave propagation in long, slender rods[2] were used to judge the convergence of the numerical solution in the various calculations. After obtaining the optimal mesh size, the effects upon the changes in artificial viscosity factors were observed.

A large deformation problem was also considered, in the form of a sphere impacting a flat plate at high velocity, to assess effects of grid size and orientation on deformations, pressures, and strains in the presence of large plastic flow.

# II. APPROACH

Two numerical examples are provided to demonstrate the effects of mesh orientation and artificial viscosity upon the numerical solution.

All computational results were obtained with the EPIC-2 (Elastic-Plastic Impact Calculation in Two Dimensions) computer code,[3] a Lagrangian finite

[1] Skalak, R., "Longitudinal Impact of a Semi-Infinite Circular Elastic Bar," Trans. ASME, J. Applied Mech., Vol 24, Dec 1955, pp. 59-63.

[2] Johnson, W., Impact Strength of Materials, Crane, Russak and Co., New York, 1972, pp. 1-12.

[3] Johnson, G. R., "EPIC-2, A Computer Program for Elastic-Plastic Impact Calculations in Two Dimensions Plus Spin," Honeywell, Inc., Defense Systems Division, Contract Report ARBRL-CR-00373, June 1978 (AD# A058786).

element formulation where constant strain triangles are used to represent a continuum, and the hydrostatic pressure in a given element is computed using the Mie-Gruneisen equation of state. The code treats problems involving wave propagation and elastic-plastic flow. It is arranged to provide solutions for projectile-target impacts and explosive detonation problems.

Material properties used for the numerical computations are given in Table 1.

Table 1. Material Properties

|  |  | Steel (Mar-M-300) | Aluminum (7075-T6) |
|---|---|---|---|
| Density | (kg/M$^3$) | 7855.00 | 2784.00 |
| Shear Modulus | (GPa) | 79.57 | 27.51 |
| Yield Stress | (GPa) | 2.07 | 0.29 |
| Ultimate Stress | (GPa) | 2.07 | 0.32 |

The propagation of elastic waves in a steel bar has been studied to ascertain the effects of mesh orientation and artificial viscosity on the numerical solution by comparison with analytical solutions. The analytical solutions assume a semi-infinite bar. The calculations presented herein are for a long bar, length-to-diameter ratio of 50. Comparisons between the computational results and the analytical solutions are made before the arrival of any reflected waves from the rear surface. Thus, the finite length bar modeled was effectively a semi-infinite bar at the times at which the comparisons are made. The elastic impact simulation involves a bar of circular cross-section made of high-hard steel. The length of the bar is 12.7 cm and the diameter is 0.254 cm. The bar impacts a rigid wall with a striking velocity of 3.048 m/sec.

In the numerical simulation of the elastic bar, a grid of quadrilateral elements comprised of four triangles per quadrilateral was used. Various spatial discretizations, such as element aspect ratio and the number of elements across the bar's radius, have been studied. The elementary one-dimensional wave equation and the approximate theory for determining how elastic stress waves propagate in infinite bars, given by Richard Skalak, are compared with the computational results in Section III.

The elementary one-dimensional linear wave equation is

$$\frac{\partial^2 u}{\partial t^2} = c^2 \frac{\partial^2 u}{\partial z^2} \, ,$$

(1)

where u is the displacement along the z axis of the bar. The constant, c, is the elementary wave velocity for a bounded medium and is given by

$$c = \sqrt{\frac{E}{\rho}} \qquad (2)$$

and the exact dilatational wave velocity in an infinite elastic medium is

$$c = \sqrt{\frac{E(1 - \nu)}{(1 - \nu)(1 - 2\nu)\rho}} \, , \qquad (3)$$

where $\nu$ is Poisson's ratio, E is Young's Modulus, and $\rho$ is the density. According to the elementary theory, a pulse propagates along the bar without changing its shape. The general form of the wave solution is

$$u = f(z - c,t) + g(z + c,t) \, . \qquad (4)$$

The specific shape of the wave is determined by the form of f. Since the wave velocity, c, is constant for an ideal one-dimensional elastic medium, the shape of the wave does not change during propagation. The equation of motion given in (1) is valid for wave propagation in slender bars (length-to-diameter ratio of at least 10) and neglects the effects of transverse strain, lateral inertia, body forces, and dissipative forces. However, the equation can be applied with reasonable success to problems where the longest wavelength is six to ten times greater than the typical cross-sectional dimension of the bar.

The analysis of the transmission of waves in a uniform circular cylinder of finite length is complex because of the introduction of the end conditions on the bar. Richard Skalak has obtained a solution, which includes transverse strain effects, for elastic wave propagation in a semi-infinite elastic bar subjected to a suddenly applied impulse through the superposition of two parts, namely

$$\frac{\partial^2 U_r}{\partial t^2} = \frac{(\lambda\mu + 2\mu)}{\rho} \frac{\partial \Delta}{\partial r} + 2\mu \frac{\partial \omega_0}{\partial z} \, , \qquad (5)$$

$$\frac{\partial^2 U_z}{\partial t^2} = \frac{(\lambda + 2\mu)}{\rho} \frac{\partial \Delta}{\partial z} - \frac{2\mu}{r} \frac{\partial}{\partial r}(r\omega_0) \, , \qquad (6)$$

11

where

$$\Delta = \frac{1}{r} \frac{\partial(rU_r)}{\partial r} + \frac{\partial U_z}{\partial z} \quad ,$$

(7)

$$\omega_0 = \tfrac{1}{2} \left( \frac{\partial u_r}{\partial z} - \frac{\partial u_z}{\partial r} \right) \quad ,$$

(8)

and

$$c^2 = \frac{\lambda + 2\mu}{\rho} \quad .$$

(9)

Skalak's solution is valid for late times at points far away from the point of application of the load and is obtained in terms of Airy's integral. The approximate solution is of the form

$$u_z' = \frac{-\nu}{c} \left[ \frac{1}{6} + \int_0^{\alpha'} Ai(\alpha)d\alpha + \frac{1}{6} + \int_0^{\alpha''} Ai(\alpha)d\alpha \right] \quad ,$$

(10)

where $\nu$ is Poisson ratio, $\alpha'$ and $\alpha''$ are the non-dimensional coordinates which measure the distance at any point along the wavelength, with respect to velocity, and $\int Ai(\alpha)d\alpha$ is Airy's integral with respect to $\alpha$, a function of time. Figure 1 depicts Skalak's refinements to the elementary theory solution. These solutions provide a guide to the reliability and accuracy of the numerical simulations.

When dealing with numerical solutions to iact problems, difficulties arise when shock waves are present. Von Neuman and Richtmyer first introduced artificial viscosity[4] in order to treat problems involving physical and mathematical discontinuities in a continuum. Their one term formulation,

$$q_1 = c_0^2 \, \rho(\Delta x)^2 \left( \frac{\partial \dot{x}}{\partial x} \right)^2$$

(11)

where $q_1 = 0$ for $\partial\dot{x}/\partial x$ greater than or equal to zero smears the shock front over several mesh widths, thus changing the discontinuities into steep but continuous wavefronts which can be treated in the context of continuum mechanics.

Later on, it was found that many finite difference discretizations tended to introduce spurious wave motions into the numerical computations. In order

---

[4] Wilkins, M. L., "Use of Artificial Viscosity in Multi-Dimensional Fluid Dynamic Calculations," *Journal of Comp. Physics*, Vol 36, No. 3, July 15, 1980.
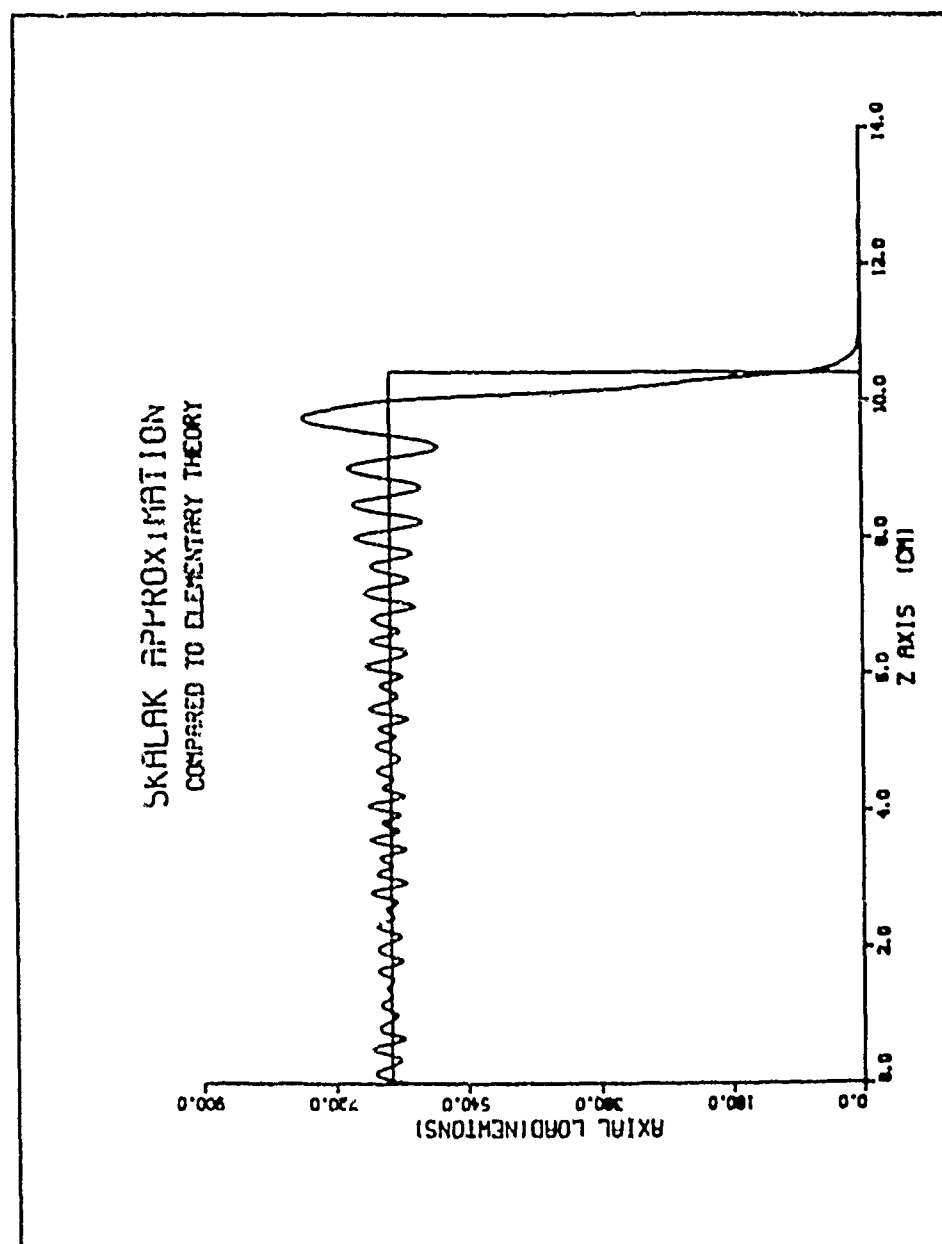
Figure 1. Richard Skalak's Analytical Solution.

to suppress these, the artificial viscosity concept of Von Neuman and Richtmyer was extended to include a second term,

$$q_2 = \alpha_1 \frac{\partial \dot{x}}{\partial x} \qquad (12)$$

$$\alpha_1 = (k_2)^2 \rho (\Delta x)^2 \left| \frac{\partial \dot{x}}{\partial x} \right| \qquad (13)$$

and $q_2 = 0$ for $\partial \dot{x}/\partial x$ greater than or equal to zero. The main purpose of the second term was to suppress numerical noise as the shock wave propagates. For computations involving solids where the sound speed exists even at zero pressure, the linear and quadratic terms are used together. Hence, the generalized form is

$$q = k_1 \rho c \Delta x \left| \frac{\partial x}{\partial x} \right| - k_2^2 \rho (\Delta x)^2 \left| \frac{\partial x}{\partial x} \right| \left| \frac{\partial x}{\partial x} \right| \qquad , \qquad (14)$$

where c is the sound speed, $\Delta x$ is the characteristic dimension in the direction of wave propagation, $\rho$ is the density, $k_1$ is the linear component, $k_2$ is the quadratic component, and x is the coordinate in the direction of motion. In EPIC-2, the generalized formula is added to the equation of state, which helps to eliminate numerical overshooting and lower level noise arising from discontinuities.

Having established the effects of irregular meshing and artificial viscosity on problems of elastic wave propagation, an additional set of simulations was undertaken to obtain an appreciation of the effect of these parameters on situations involving plastic flow. Only the mesh orientation was varied in the plastic impact study. Three mesh orientations were considered which are shown in Figure 2.

The effects of the various mesh orientations can be seen from the deformation patterns but become even more evident when strain and pressure distributions are studied. Finally, while not explicitly considered in this study, the behavior of numerical results in the presence of different failure criteria and post-failure models can be inferred from the results presented.

## III. RESULTS

A. Elastic Impact

A comparison of the results from the various computations to determine the grid size, using quadrilateral elements comprised of four triangles, gave

A.  IDIA = 1  Hypotenuse of the Triangle is drawn from the lower left hand corner to the upper right hand corner.

B.  IDIA = 2  Hypotenuse of the Triangle is drawn from the upper left hand corner to the lower right hand corner.

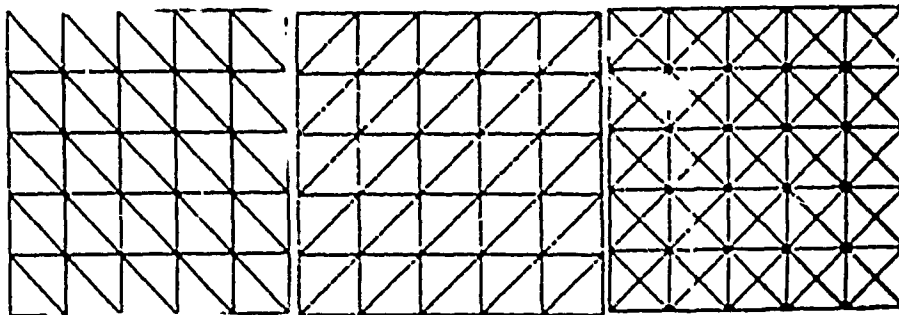C.  Quadrilateral Elements Comprised of four Triangles.

Figure 2.  Element Orientations in EPIC-2 Code.

some interesting results, as shown in Figures 3 - 14. In all six cases, the change in amplitude and time remained relatively small. Using a uniform grid and refining the mesh, there is one considerable effect: by increasing the number of nodal points and decreasing the size of the elements, the higher frequencies are resolved.

In Figures 4, 6 and 8 the wave profile in the bar at 20$\mu$s is presented for 1, 2 and 3 elements across the radius respectively. In all three cases the element aspect ratio was a constant of 1:1. Thus, as the number of elements across the radius is increased, the resolution is improved since the higher frequency waves are now being accounted for in the numerical solution. Comparison of the high resolution wave profile in Figure 8 with Skalak's solution in Figure 1 shows close agreement.

In contrast to the elementary theory solution, the wavefront predicted from both Skalak's solution and the numerical solution has a finite slope. The elementary theory reasonably approximates some features, such as peak amplitude of the behavior of long bars subjected to impulsive loading; but it is incapable of resolving some aspects of the problem. The solution implies that the waves transmitted are traveling with constant velocity and without alteration of shape. In the Skalak and numerical solutions, the oscillations arise due to transverse strain effects. They are not artificially introduced by the numerical scheme. Furthermore, as one refines the mesh, the wave profile exhibits an increase in the number of oscillations behind the wave front.

Figures 8, 10, 12 and 14 show the wave profile in the bar at 20$\mu$s for element aspect ratios of 1:1, 2:1, 3:1 and 4:1 respectively. As the aspect ratio is increased the axial resolution decreases. This decrease in axial resolution prevents the numerical solution from capturing the high frequency wave components in the axial direction. This can be observed in the plots by the decrease in the number of oscillations in the wave profile behind the wave front.

The cost of computations may often be a major factor in determining the grid size. With a large aspect ratio and a coarse grid, the CPU time and costs are relatively low. While the cost and the CPU time practically double with grid refinements. Thus, the user must make a trade off between accuracy and cost.

The effects of changes in artificial viscosity coefficients are shown in Figures 15 - 17. An increase in the linear component results in excessive distortion of the wave front and a decrease in the oscillations occurring along the wavelength. The effect of changes in the quadratic coefficient is small. This is primarily because the quadratic component dissipates more rapidly away from the shock than the linear component.

B. Plastic Impact

An additional set of simulations has been performed to gain an appreciation for the effect of element orientation on the numerical solution of impacts involving plastic flow. In this set of computations the mesh orientation, in the target only, was altered. All computations were
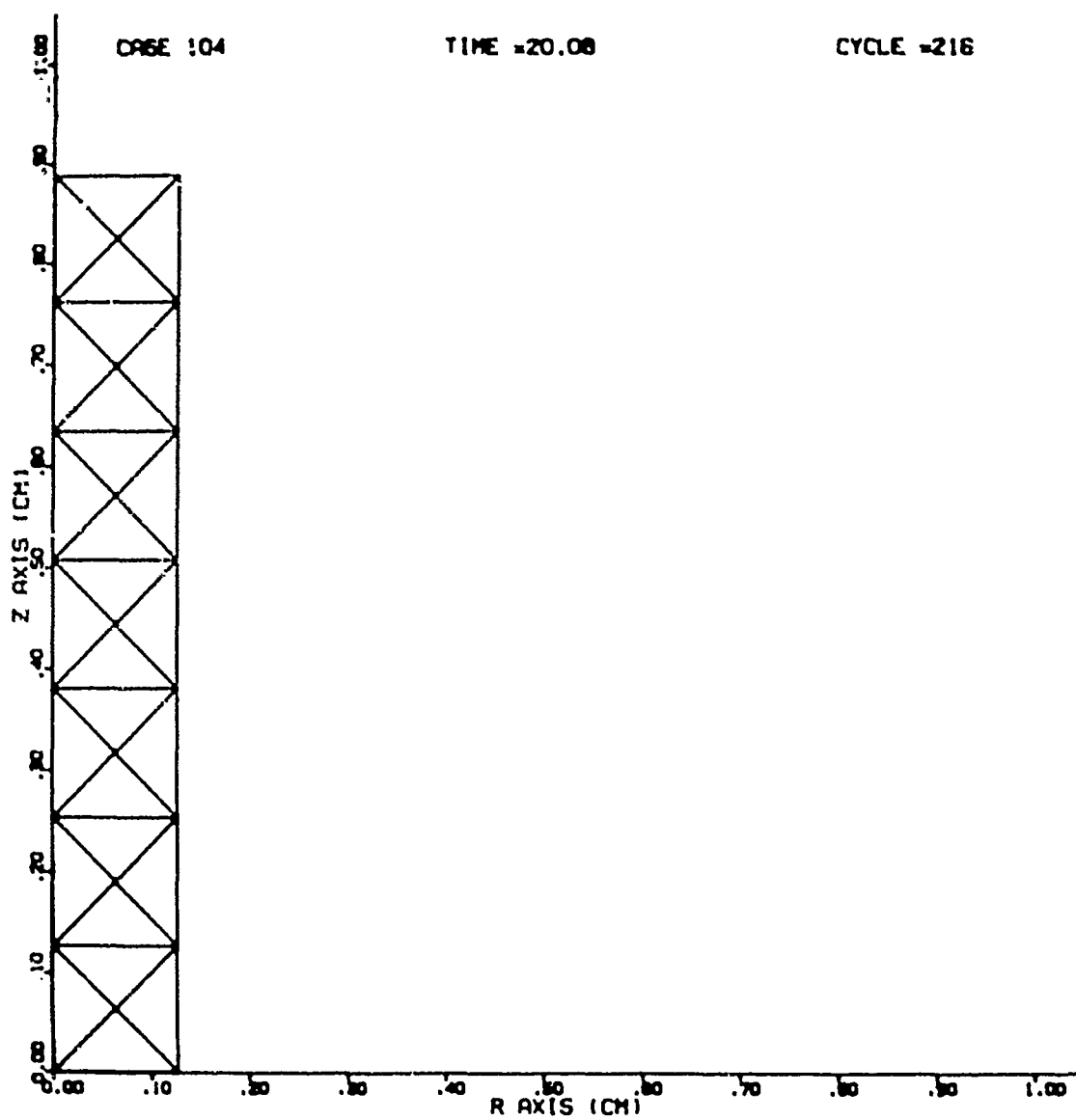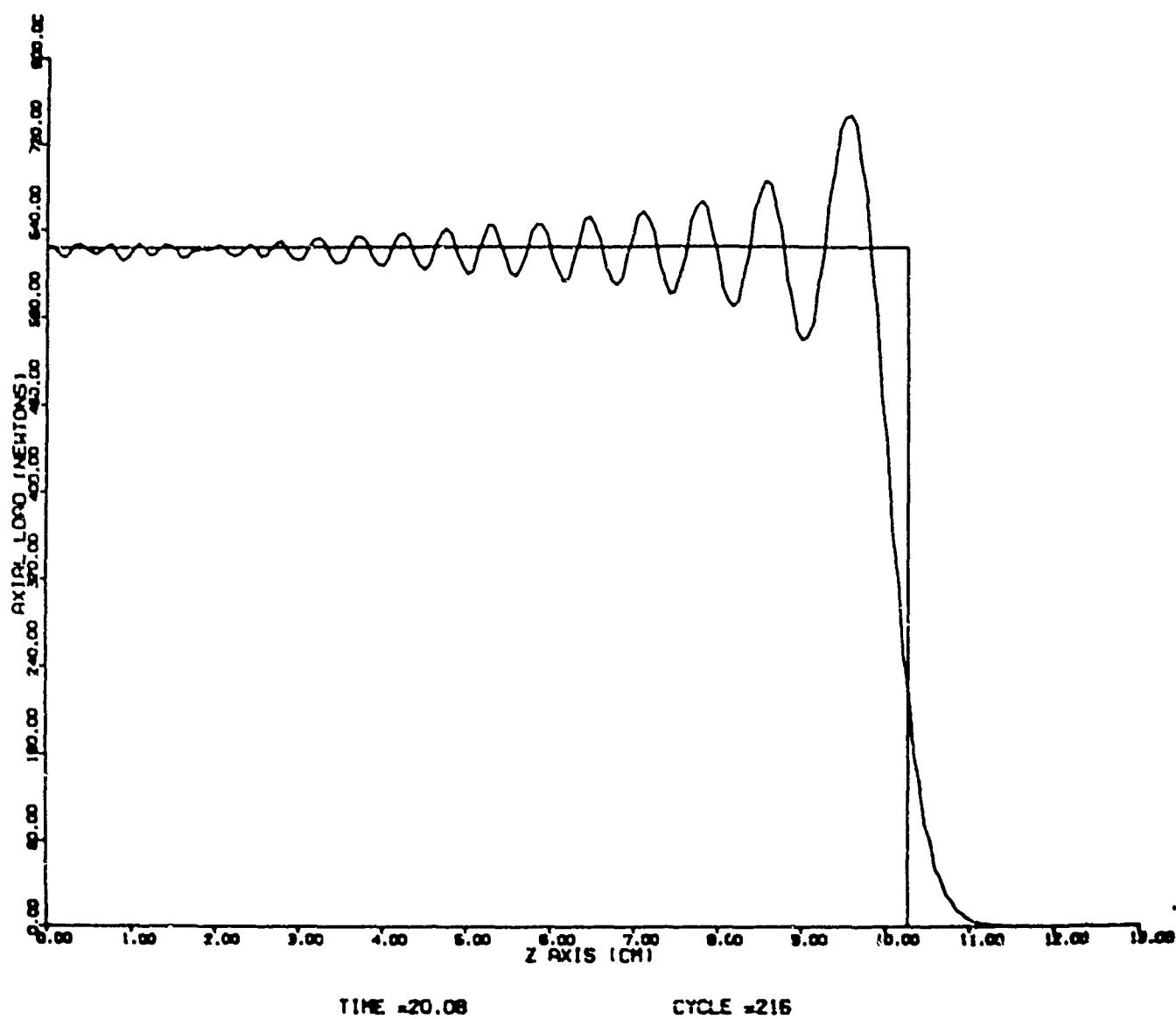
16

Figure 3.  Computational Grid Map, 400 Elements.

AXIAL LOAD (NEWTONS)

Z AXIS (CM)

TIME =20.08          CYCLE =216

Figure 4.   Load/Displacement in Bar, Aspect Ratio  1-1, Case 104.

18

CASE 103　　　　　　　TIME =20.03　　　　　　　CYCLE =389
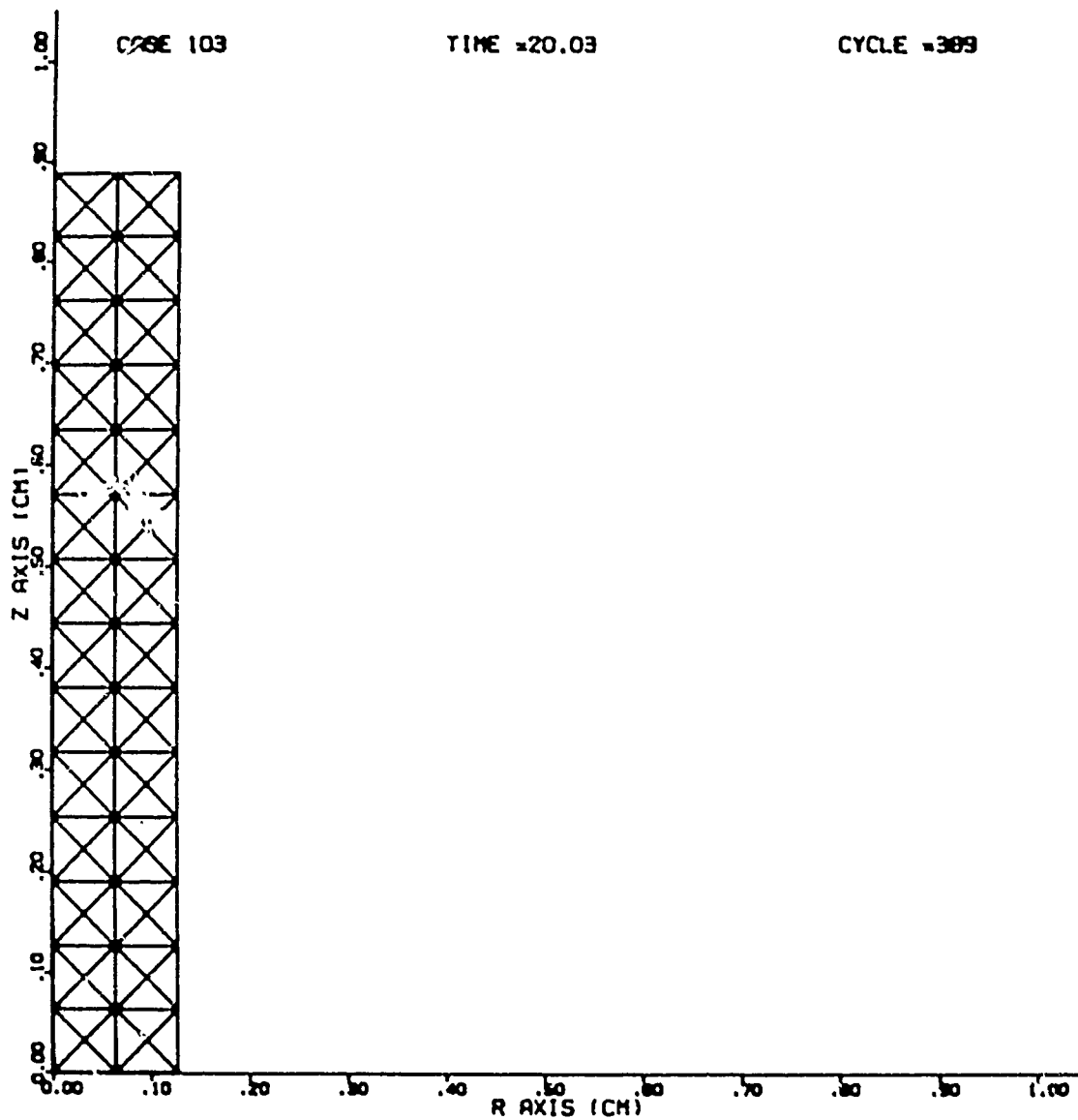
Z AXIS (CM)

R AXIS (CM)

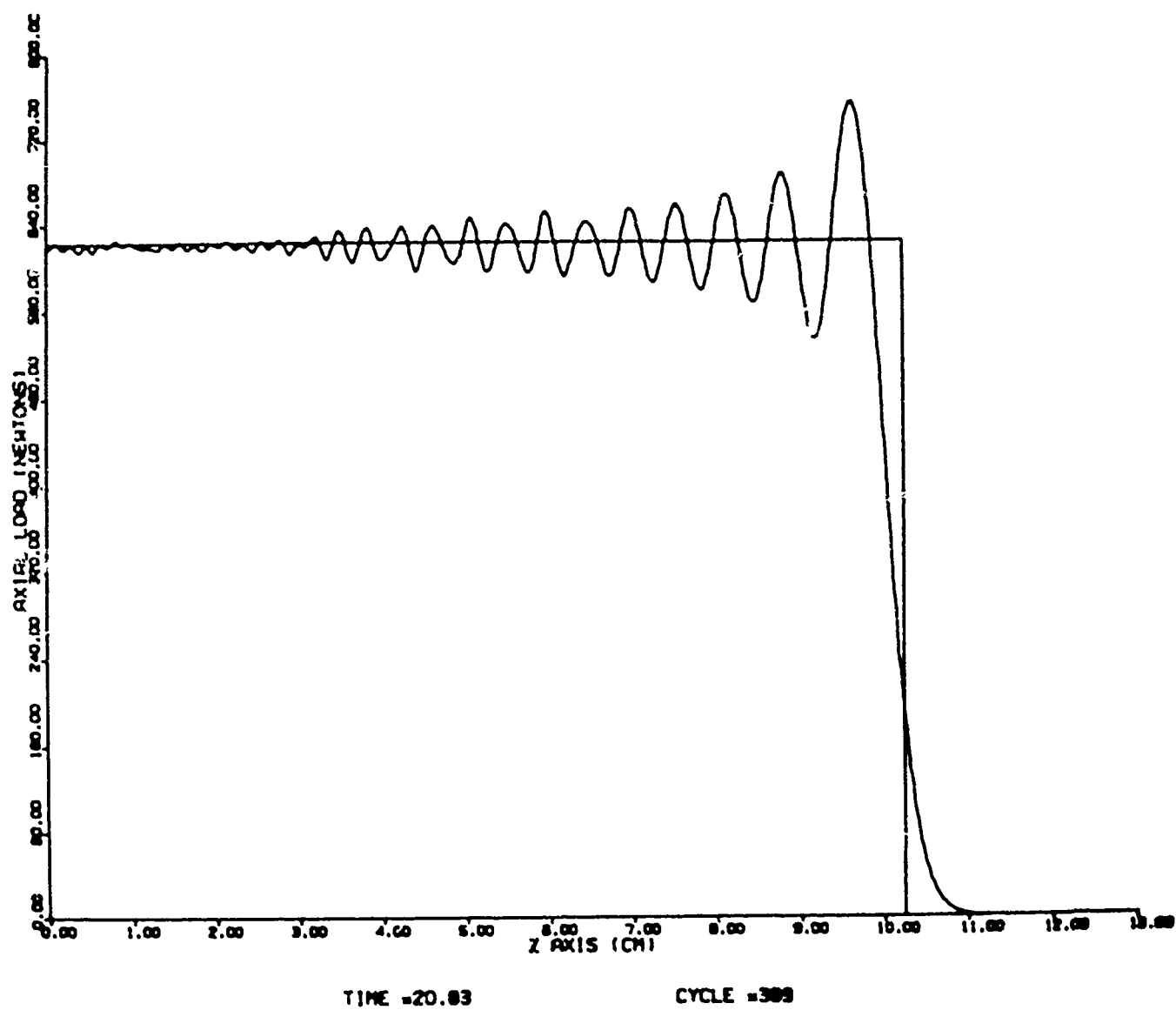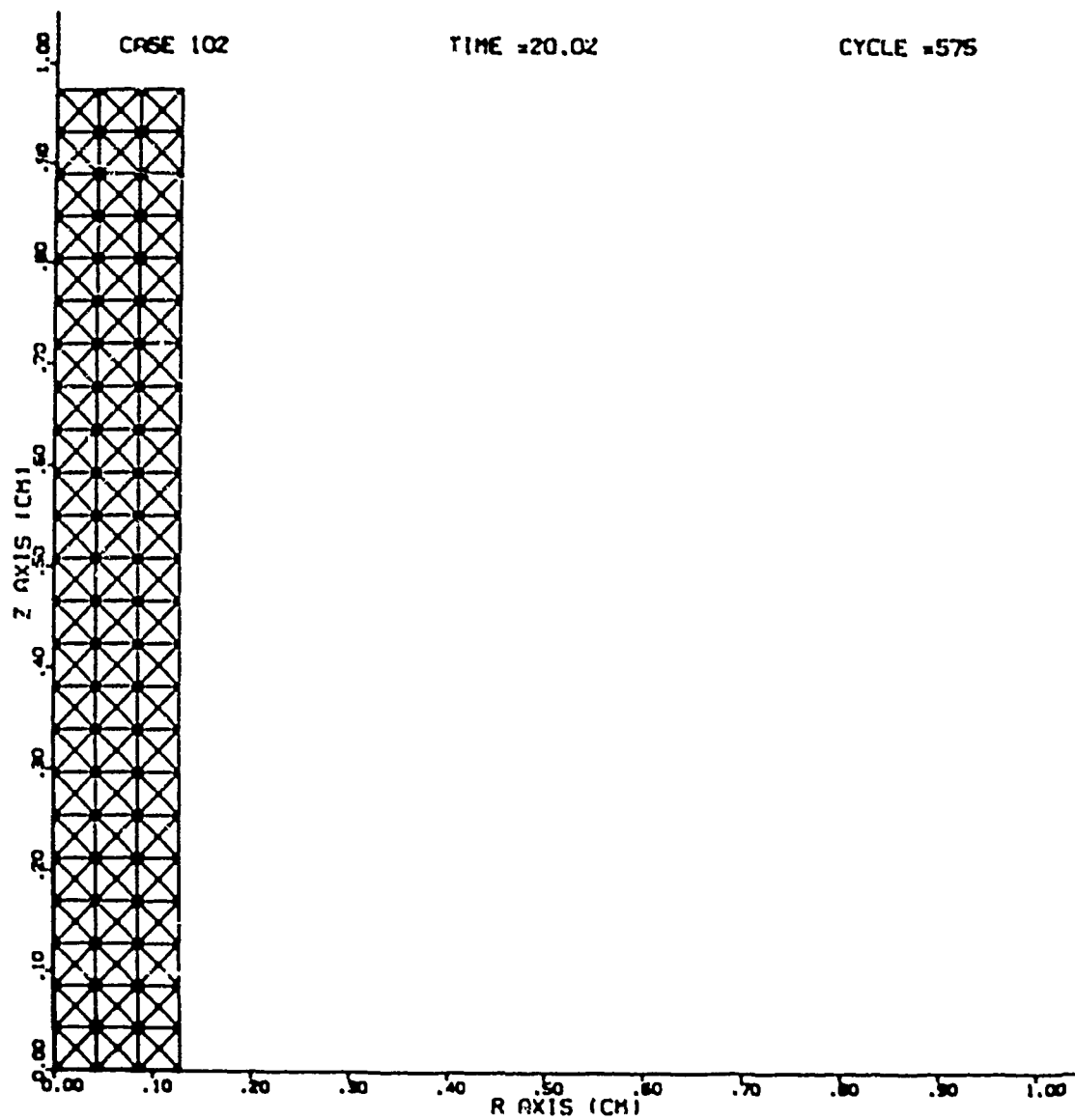Figure 5.　Computational Grid Map,　1600 Elements.

19

Figure 6. Load/Displacement in Bar, Aspect Ratio 1-1, Case 105.

20
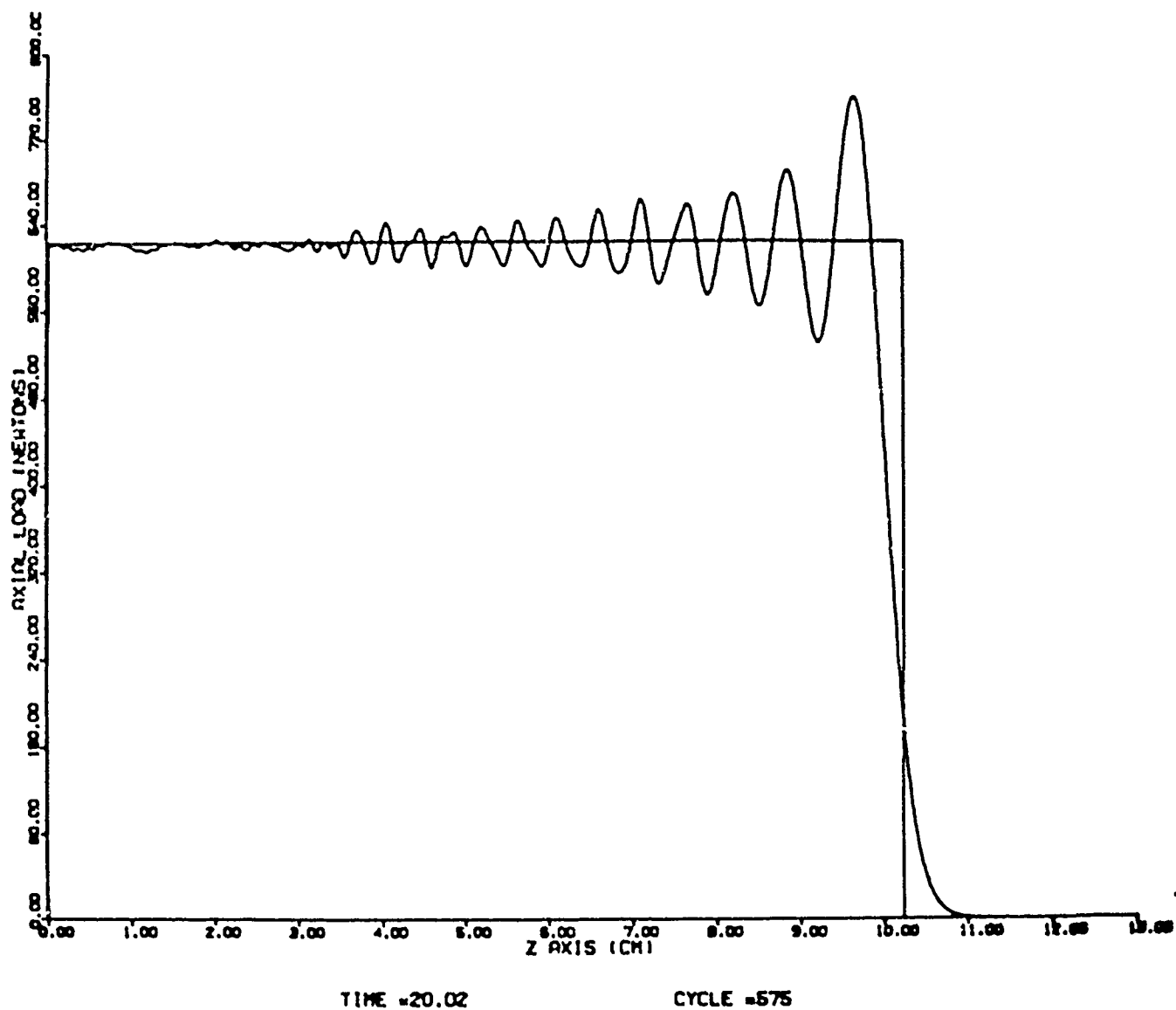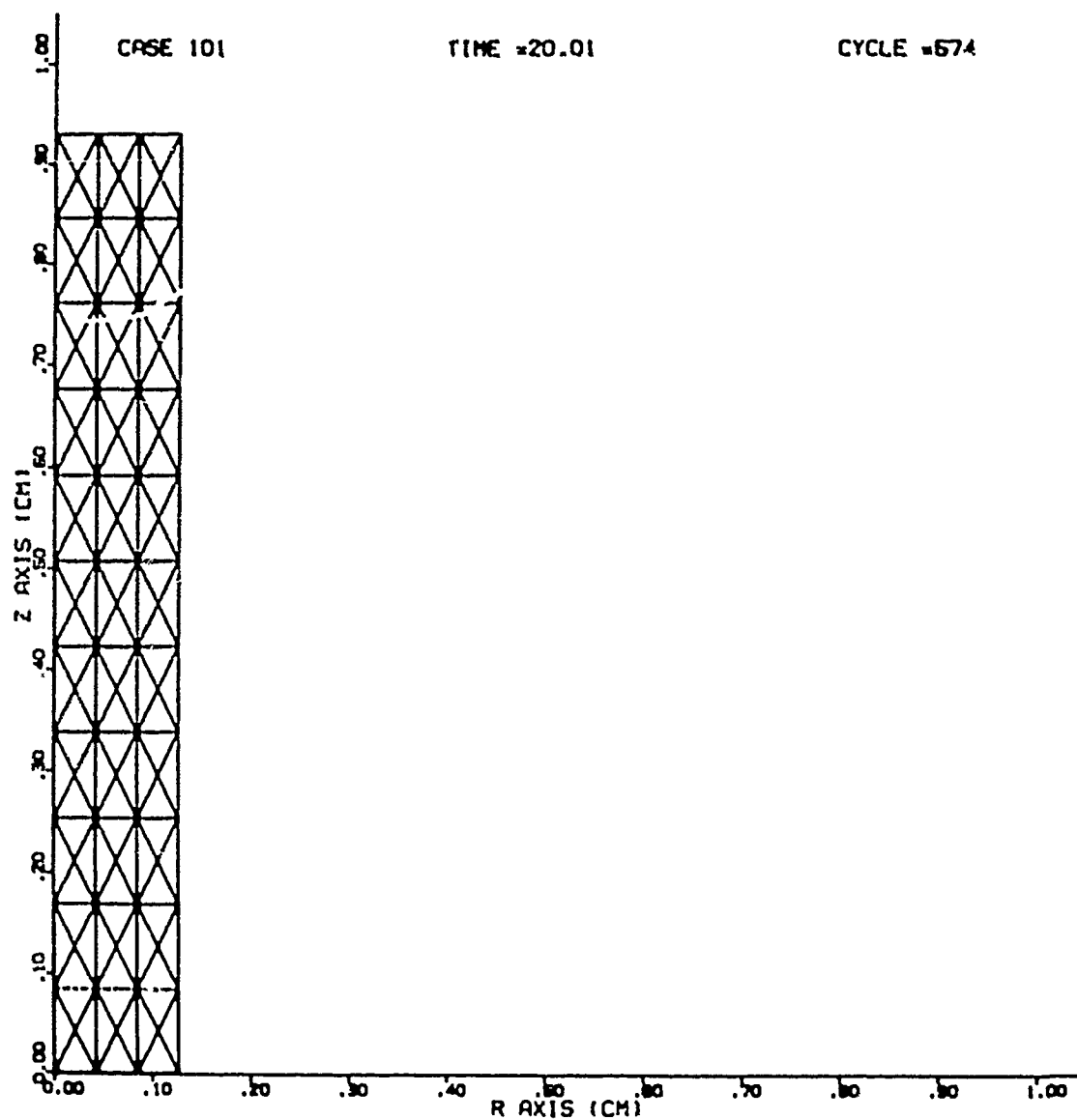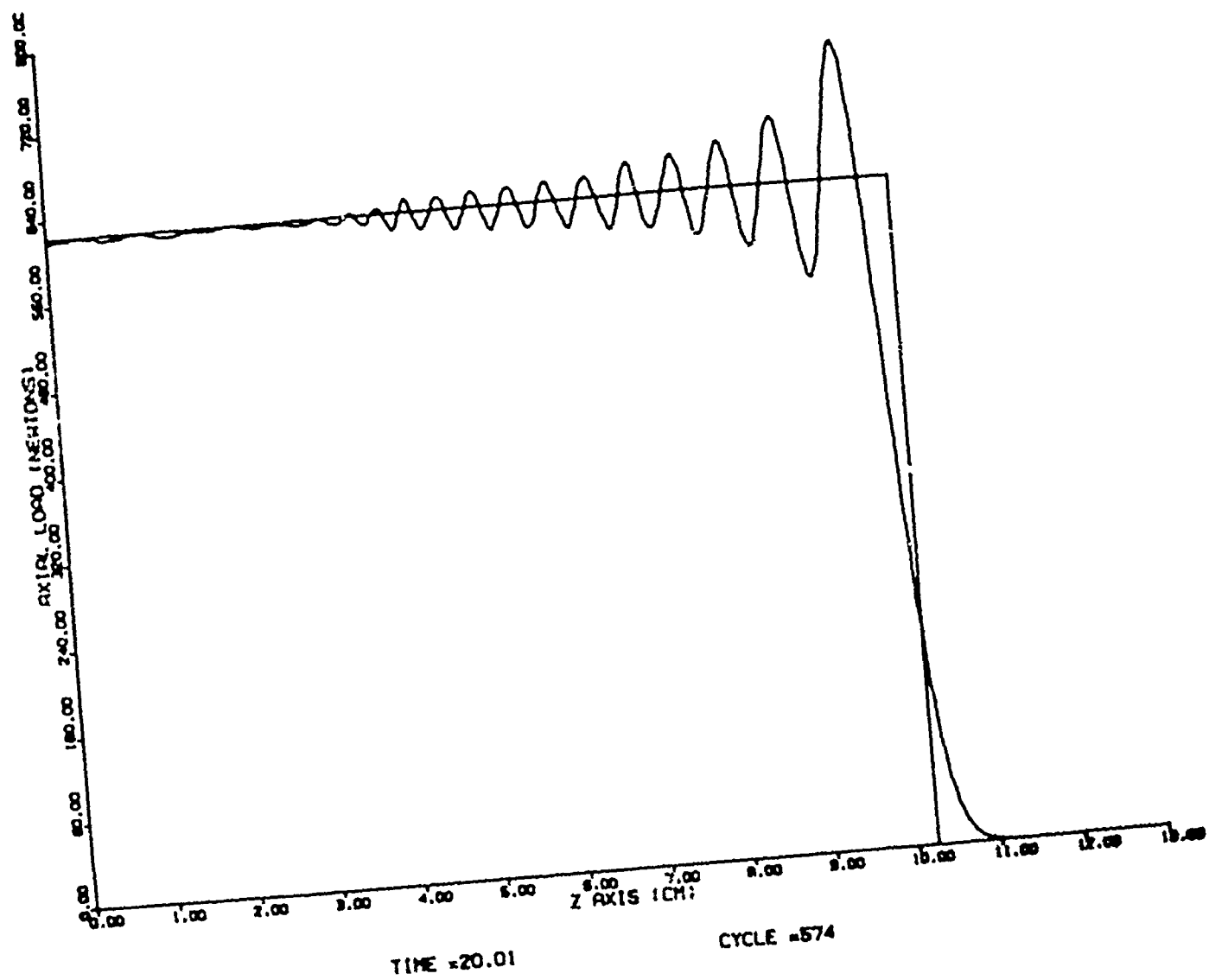
Figure 7.  Computational Grid Map, 3600 Elements.

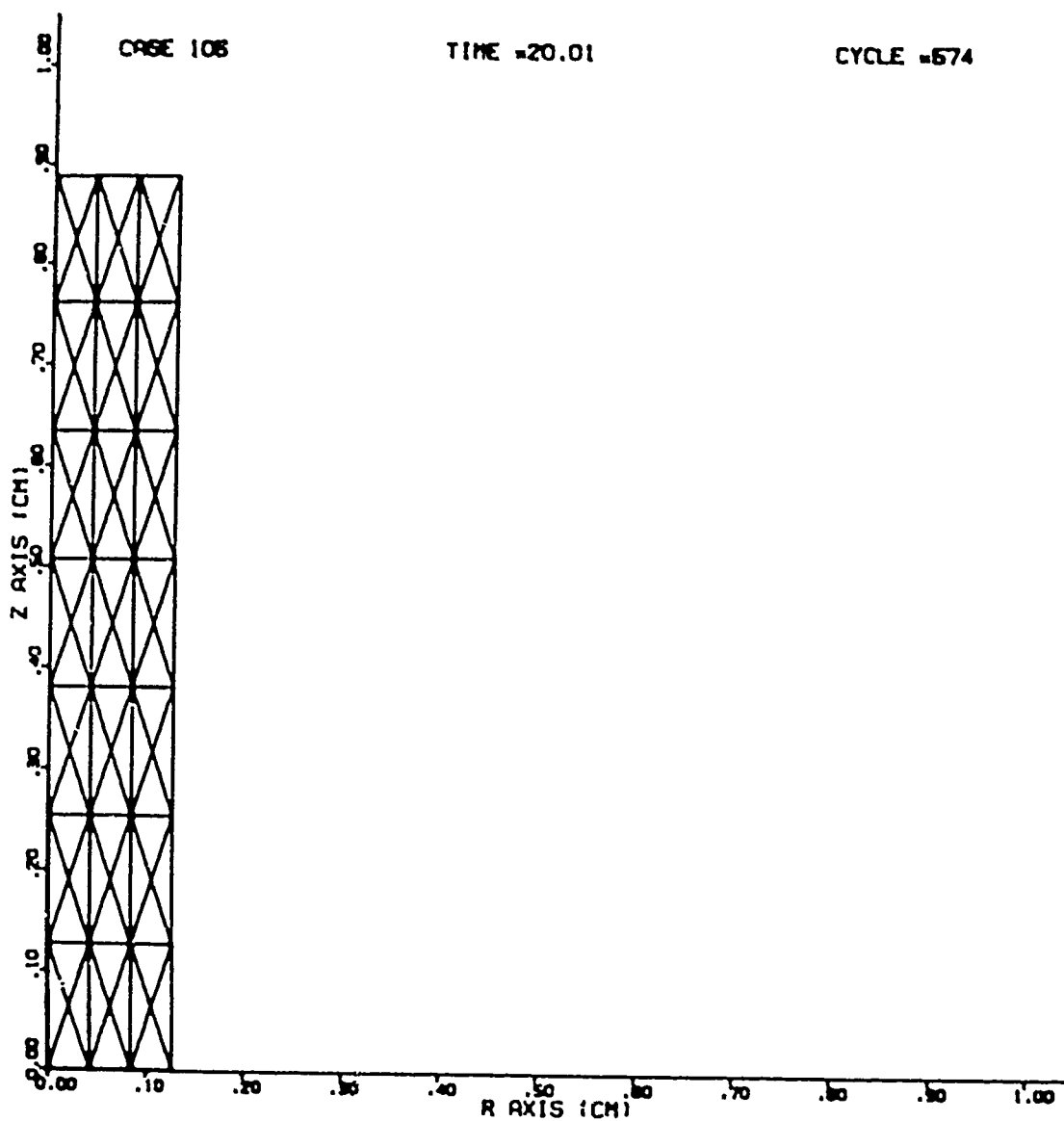Figure 8.   Load/Displacement in Bar, Aspect Ratio 1-1, Case 102.

22

CASE 101                    TIME =20.01                    CYCLE =674

Figure 9.   Computational Grid Map, 1800 Elements.

23

Figure 10. Load/Displacement in Bar, Aspect Ratio 2-1, Case 101.
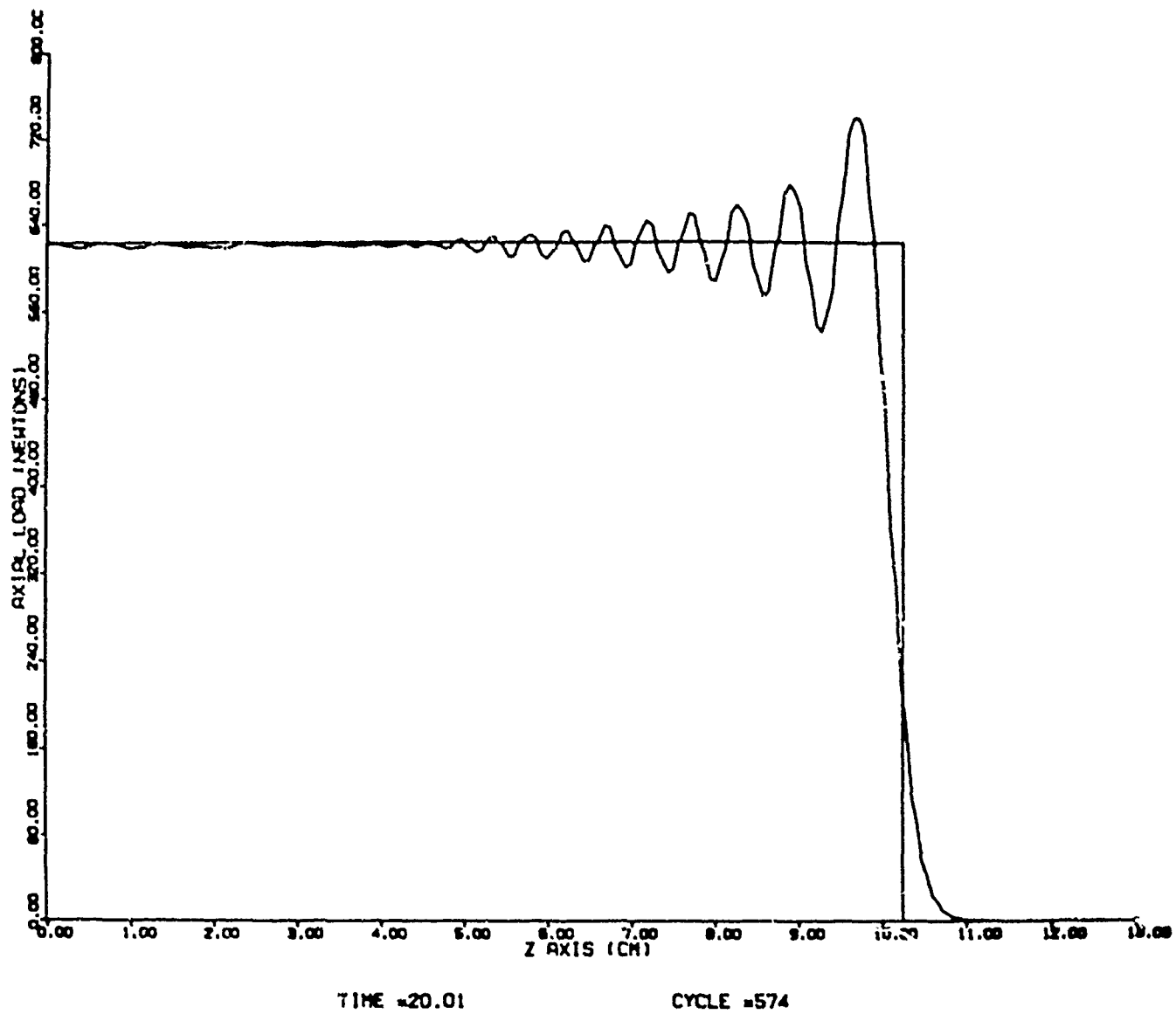
24

Figure 11.   Computational Grid Map, 1200 Elements.

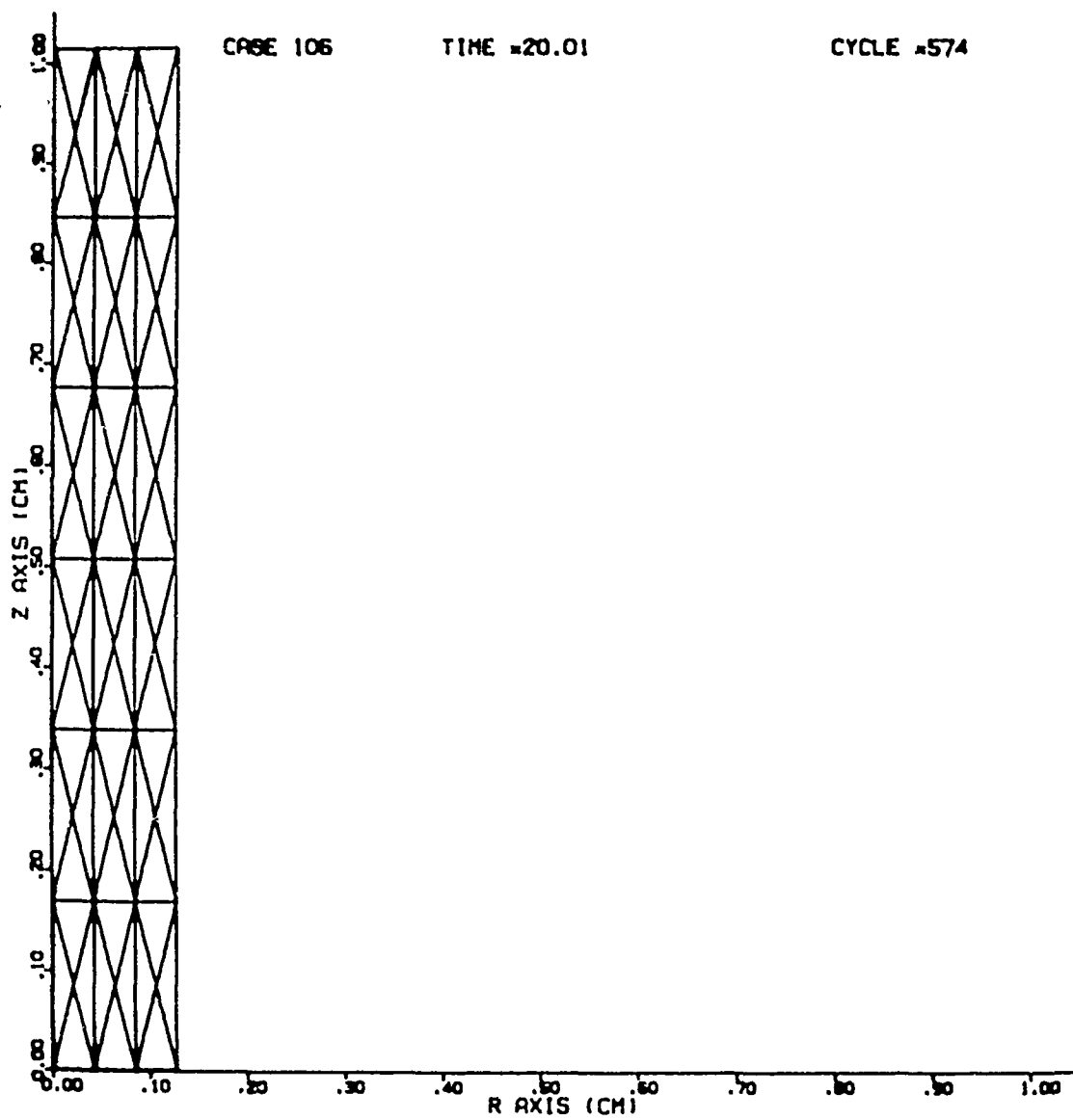Figure 12. Load/Displacement in Bar, Aspect Ratio 3-1, Case 105.

CASE 106          TIME =20.01                    CYCLE =574
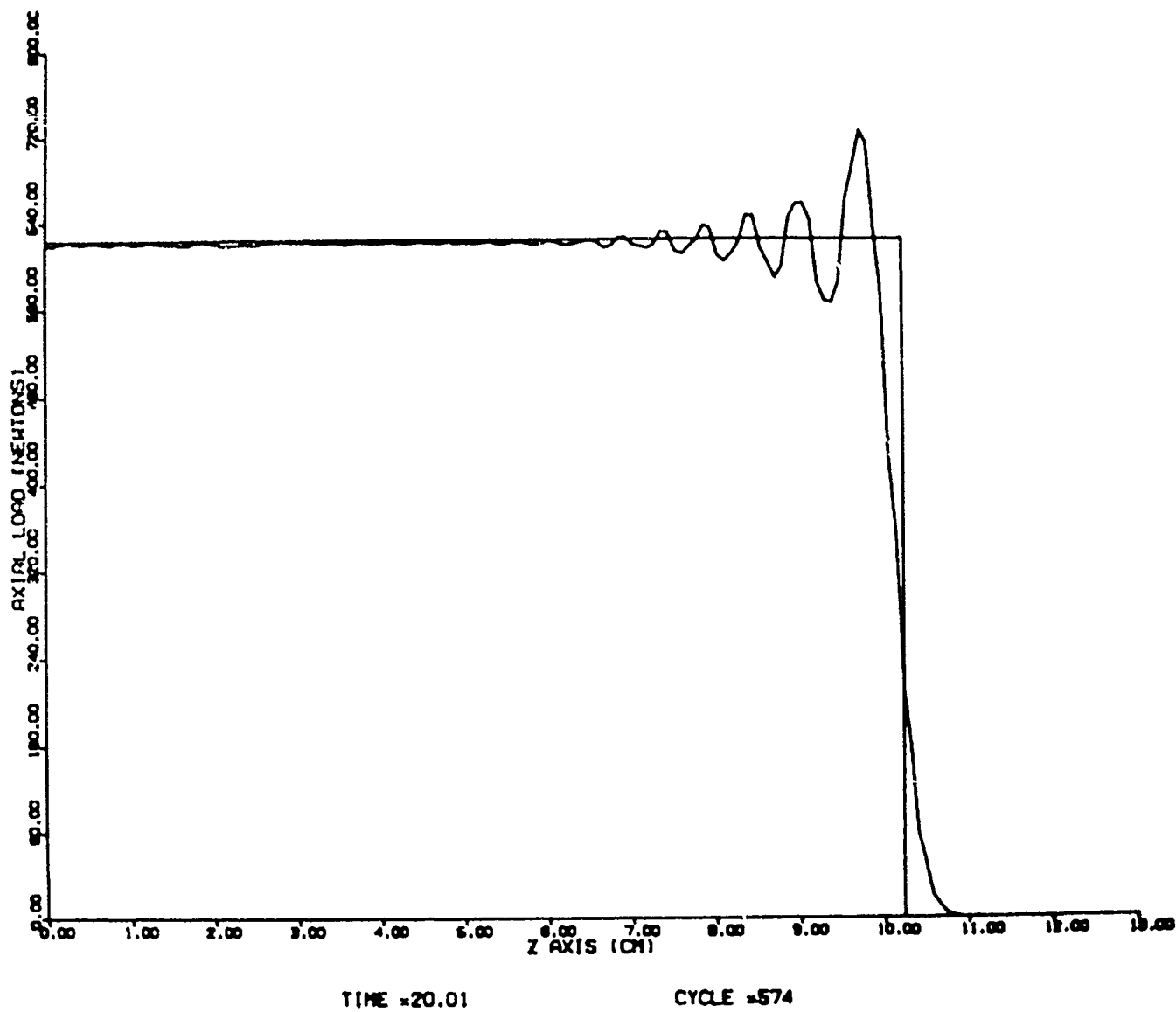
Figure 13.   Computational Grid Map, 900 Elements.

27

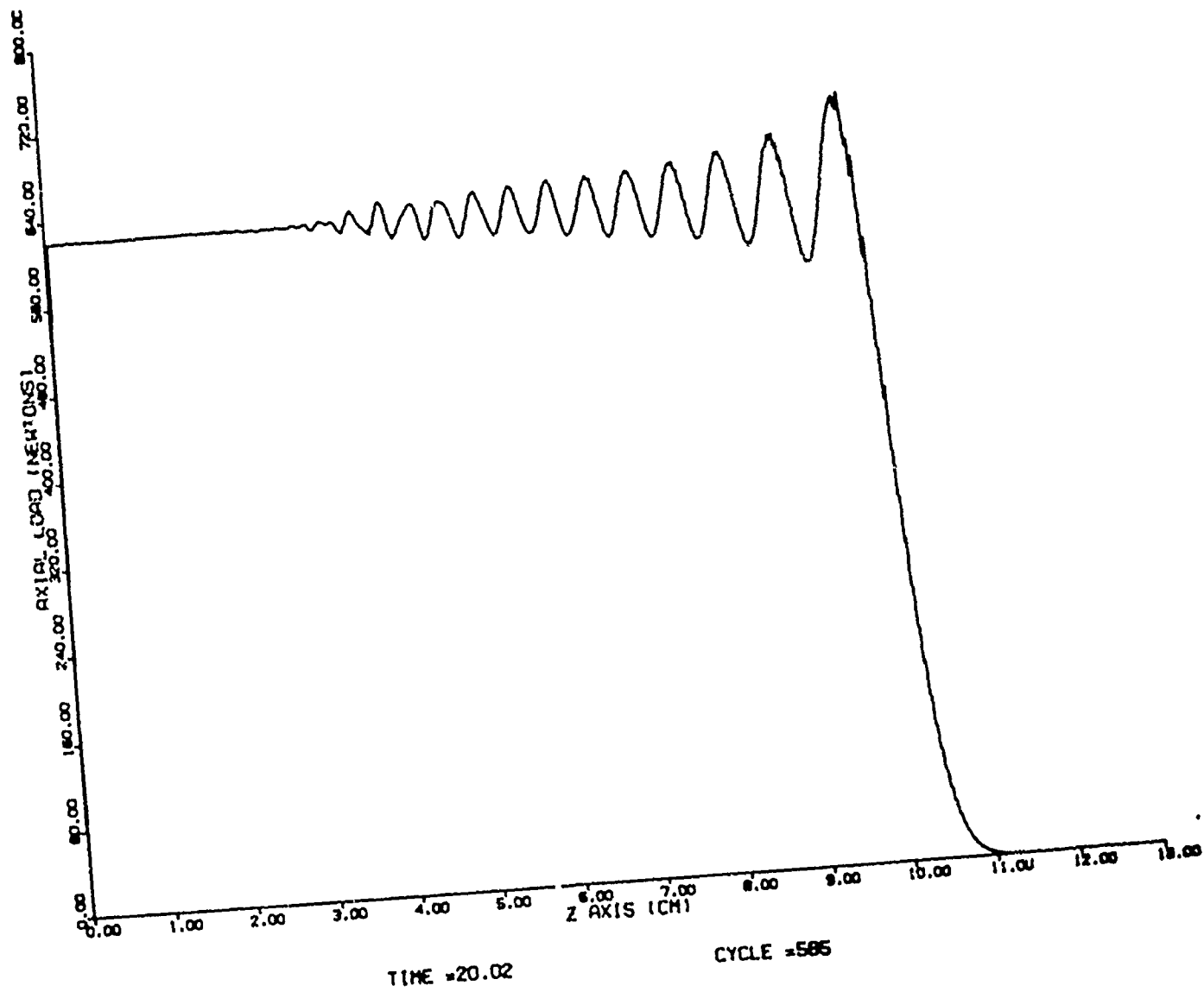Figure 14. Load/Displacement in Bar, Aspect Ratio 4-1, Case 106.

28

Figure 15. Artificial Viscosity Plot, Linear Factor 0.6, Quadratic Factor 4.0.
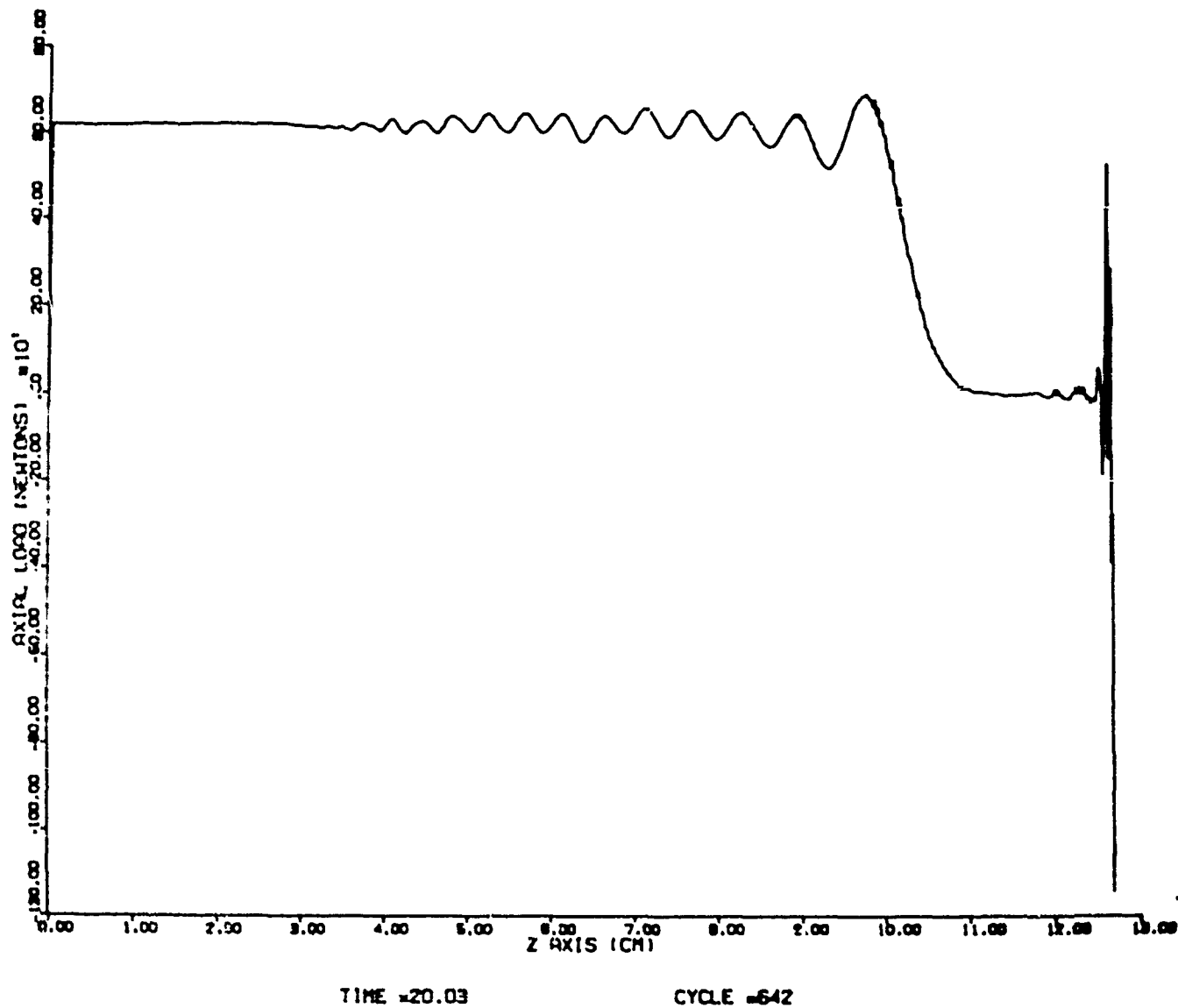
29

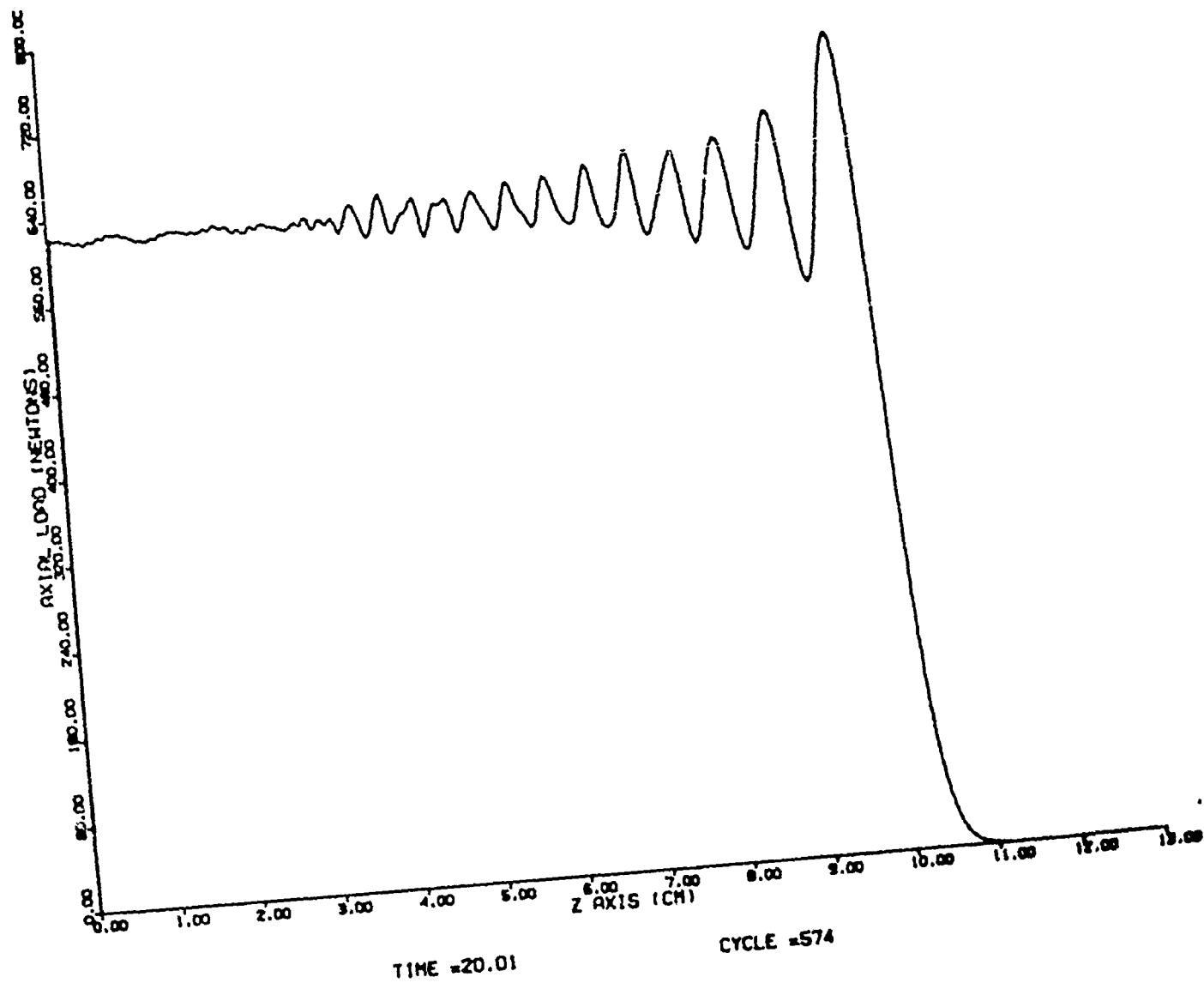Figure 16.  Artificial Viscosity Plot, Linear Factor 1.0, Quadratic Factor 4.0.

Figure 17. Artificial Viscosity Plot, Linear Factor 0.2, Quadratic Factor 2.0.

31

terminated at 10μs, at which time the problems are sufficiently advanced to obtain reasonable results. The plastic impact studied consists of a steel sphere impacting an aluminum plate with a velocity of 1524 m/sec. The target plate thickness is 5.08 cm. The first target mesh orientation studied has the diagonals oriented with a positive slope (IDIA=1 in Figure 2), see Figure 18.

Figures 19 and 20 show the computational results at 5μs and 10μs respectively. At 10μs the target is forming a V-shape which will produce unrealistic deformations of the sphere and numerical instabilities. The computational results for the diagonals oriented with a negative slope are presented in Figures 21 and 22. At 5μs there is a slight pulling of the elements in a positive direction. By 10μs the target deformation is unreasonably stiff. Clearly, from Figures 19-22, the diagonal orientation has a significant influence on the predicted deformations.

In Figures 23 and 24 the quadrilateral elements comprised of four triangles allow for large deformations to occur without introducing artificial stiffness and/or asymmetries into the calculations, which are very typical of the triangular zones.

The response of the target material has been carefully examined for strain, pressure, and distribution as well as failure patterns. Material failure in the EPIC-2 code is governed by a failure criterion based on equivalent plastic strain. When a user's specified value for this quantity in an element is exceeded, the element is considered to have partially failed, and no tensile or shear stresses are permitted. In effect, the element behaves as a fluid. Total failure at higher values of equivalent plastic strain is also permitted. In this case, neither stress nor pressure can be carried by an element, and it is therefore ignored in the computational loop. The element connectivity is destroyed, but the nodes and their associated mass and velocity are retained to conserve mass and momentum. The results pertaining to the failure of the elements in the target are shown in Appendix A. Those elements marked with an "F" have exceeded the partial failure criterion of 0.6.

With regard to the first two cases, 107 (IDIA=1) and 108 (IDIA=2), the elements are being failed far away from the impact area. The total amount of failure is small; and the dispersement of the failed elements is more widely distributed in the target, in comparison to Case 109.

Element strains are derived by integrating the strain rates, which are obtained from the geometry of the elements and the nodal velocities. The strain contours are evaluated at five different levels and are shown in Appendix B. The strain contours in Cases 107 and 108 sharply deviate from the area of impact and extend out farther into the target in comparison to Case 109.

The hydrostatic pressure is dependent on the volumetric strains and internal energy in the elements. The results from the positive and negative pressure contours are shown in Appendix C. In comparing the first two Cases to the third, the positive pressure contours are more condensed around the area of impact and the failed elements. With regard to the negative pressure fields, there is a greater magnitude of the pressure in the projectile than in
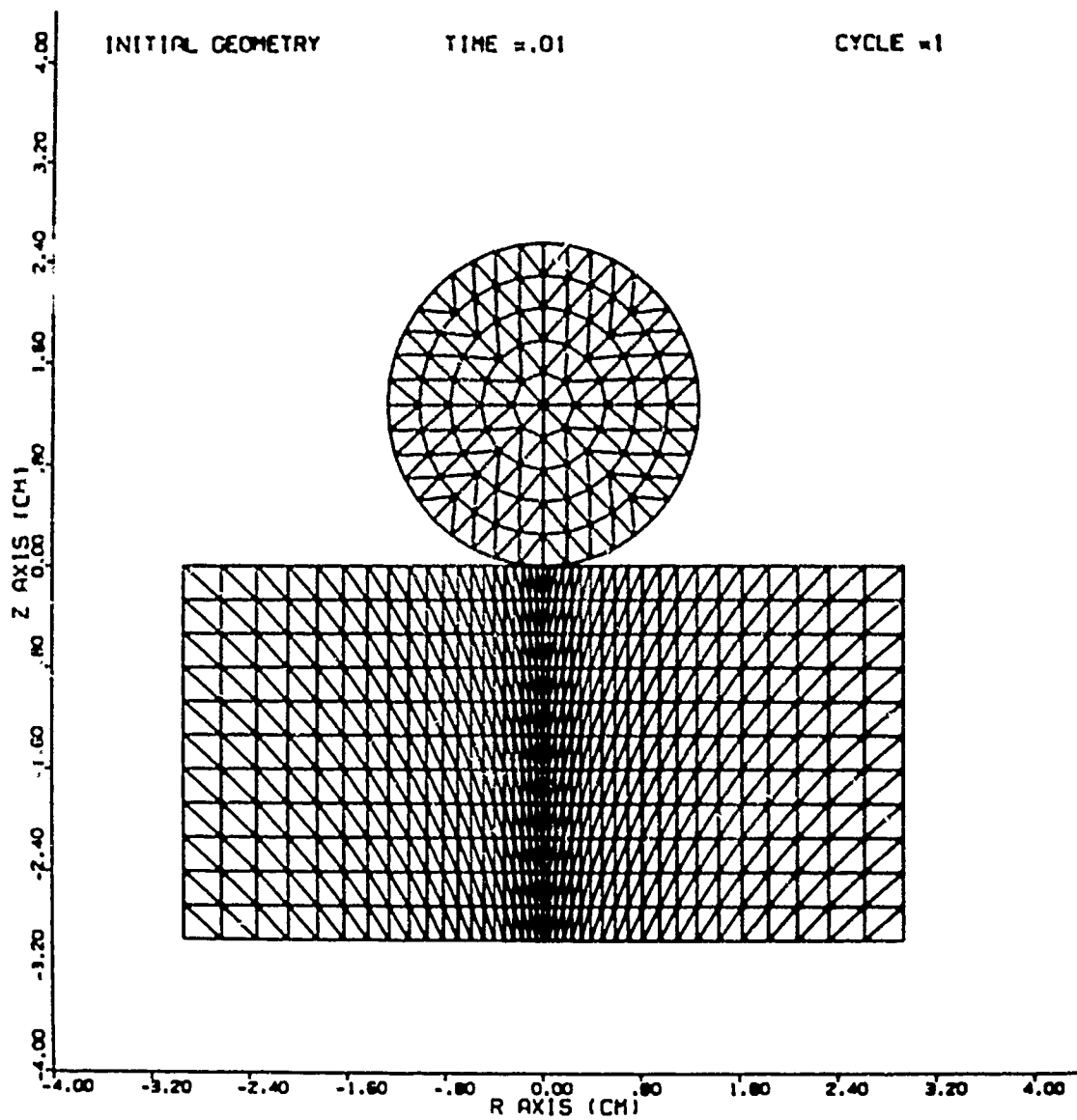
32

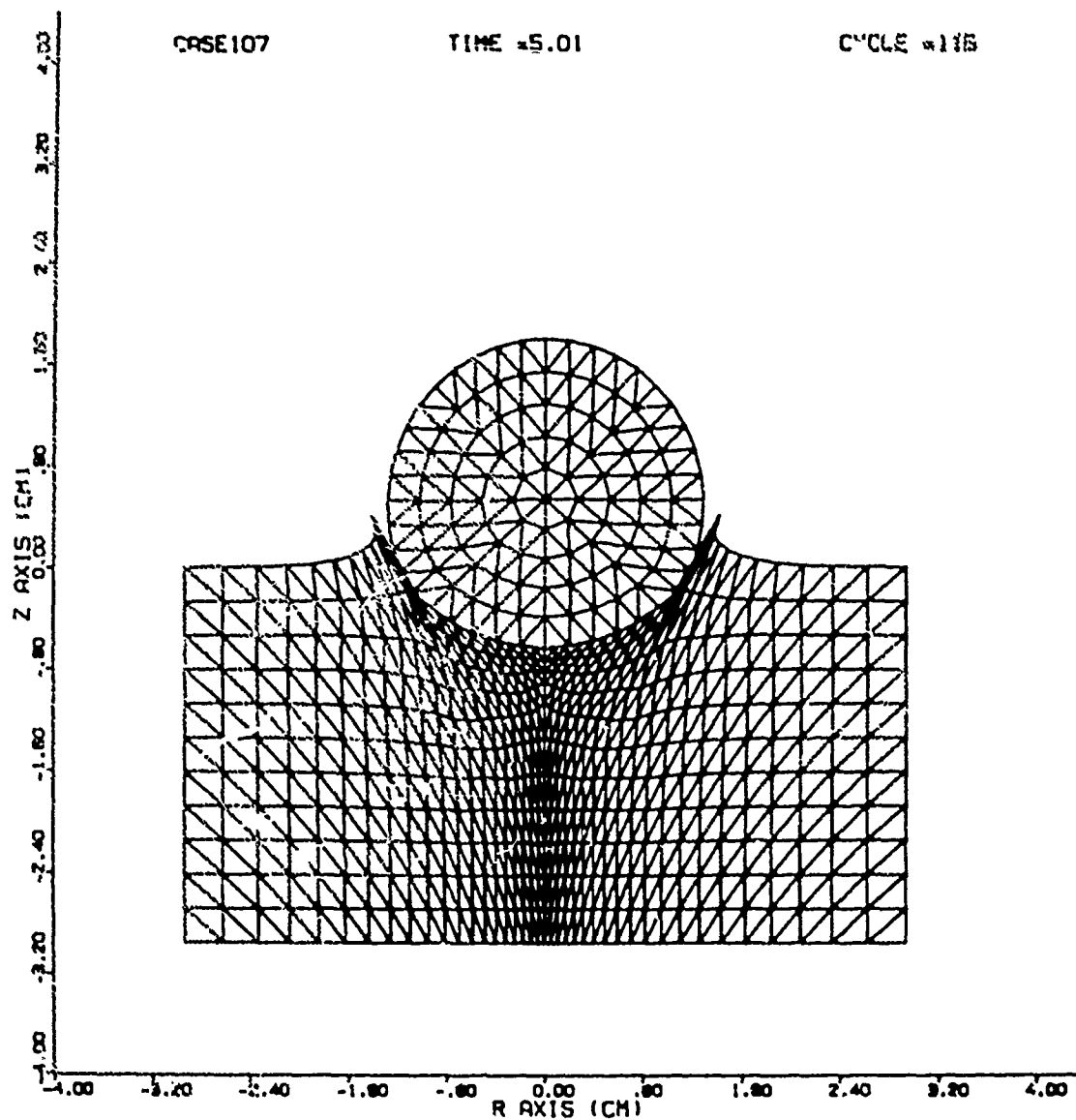Figure 18. Initial Configuration of Sphere/Plate Impact.

33

CASE107       TIME =5.01       C'CLE =116

Figure 19.    Deformation of Sphere/Plate Impact, t = 5 μs, IDIA = 1.

34

Figure 20. Deformation of Sphere/Plate Impact, t = 10 μs, IDIA = 1.
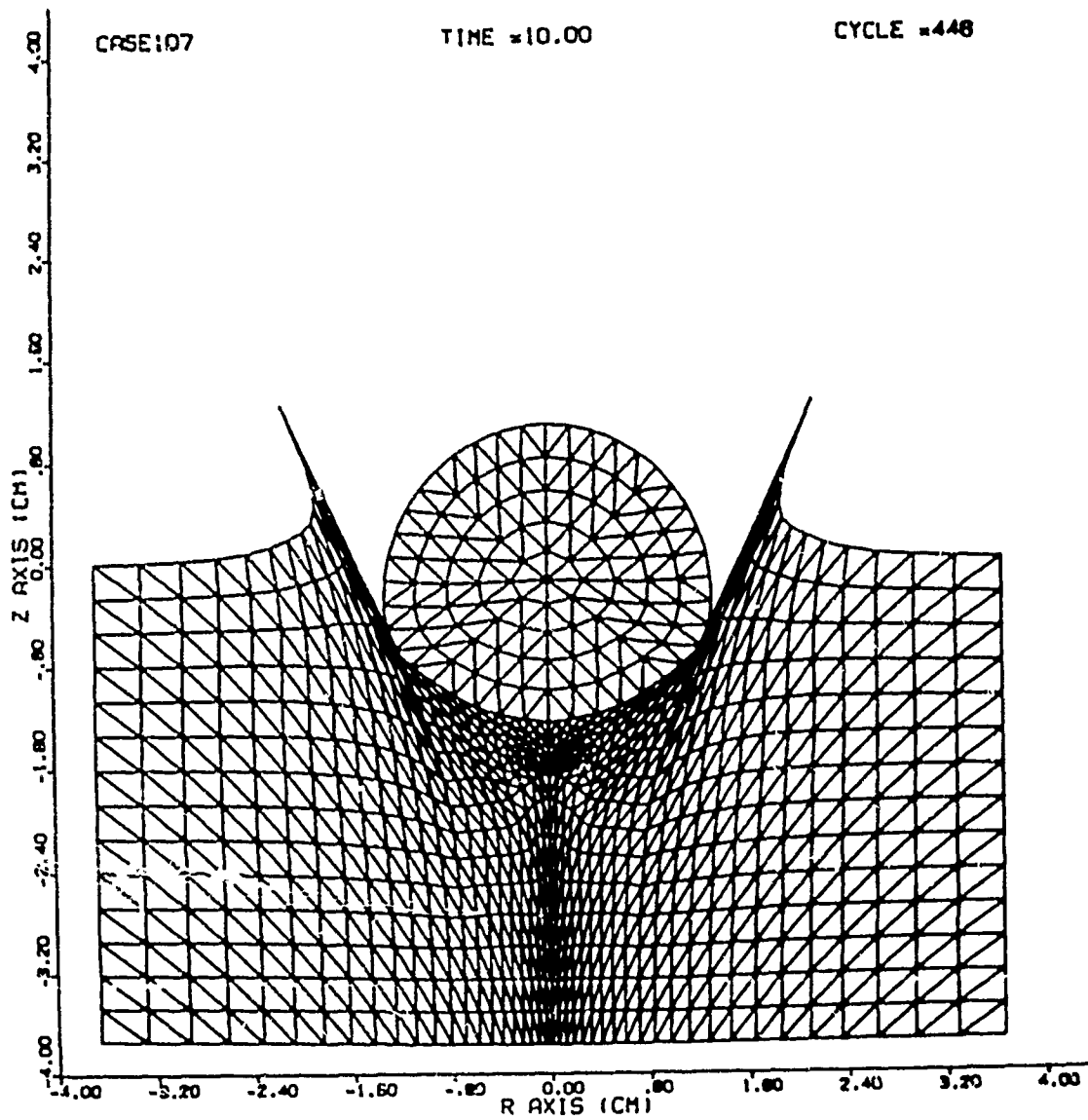
35

CASE 108          TIME = 5.01          CYCLE = 140
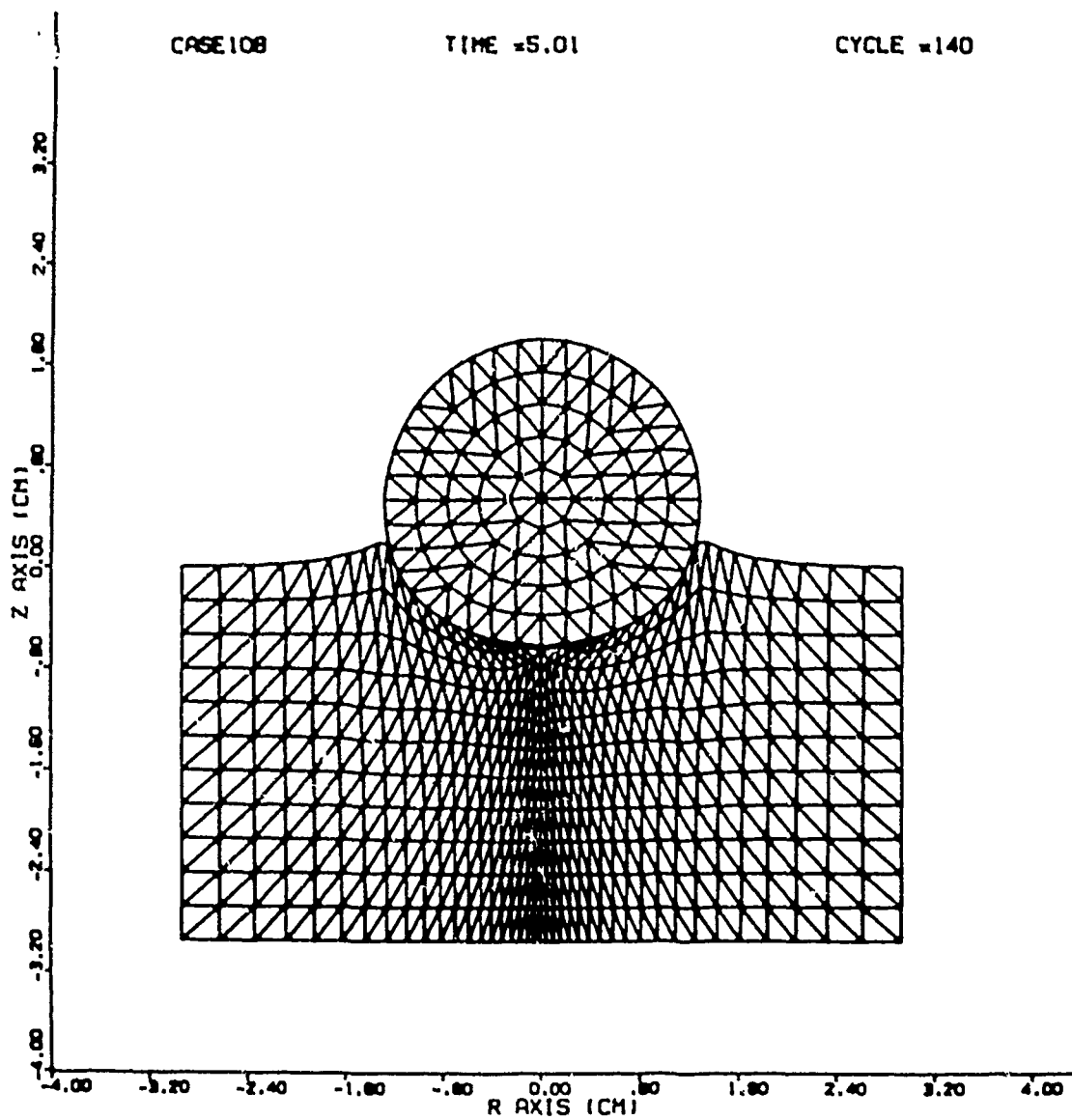
Figure 21.   Deformation of Sphere/Plate Impact, t = 5 μs, IDIA = 2.

36
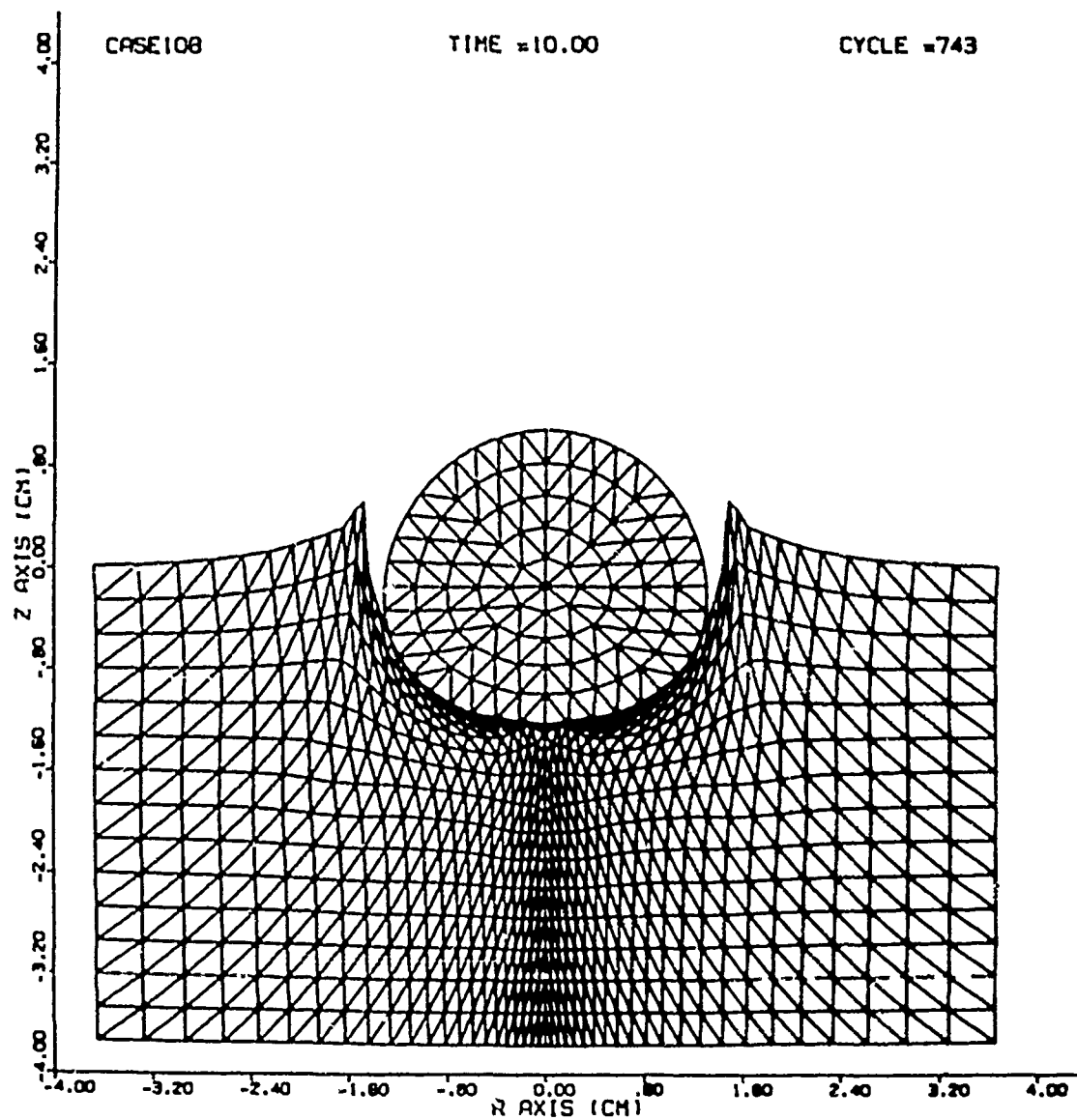
Figure 22. Deformation of Sphere/Plate Impact, t = 10 μs, IDIA = 2.
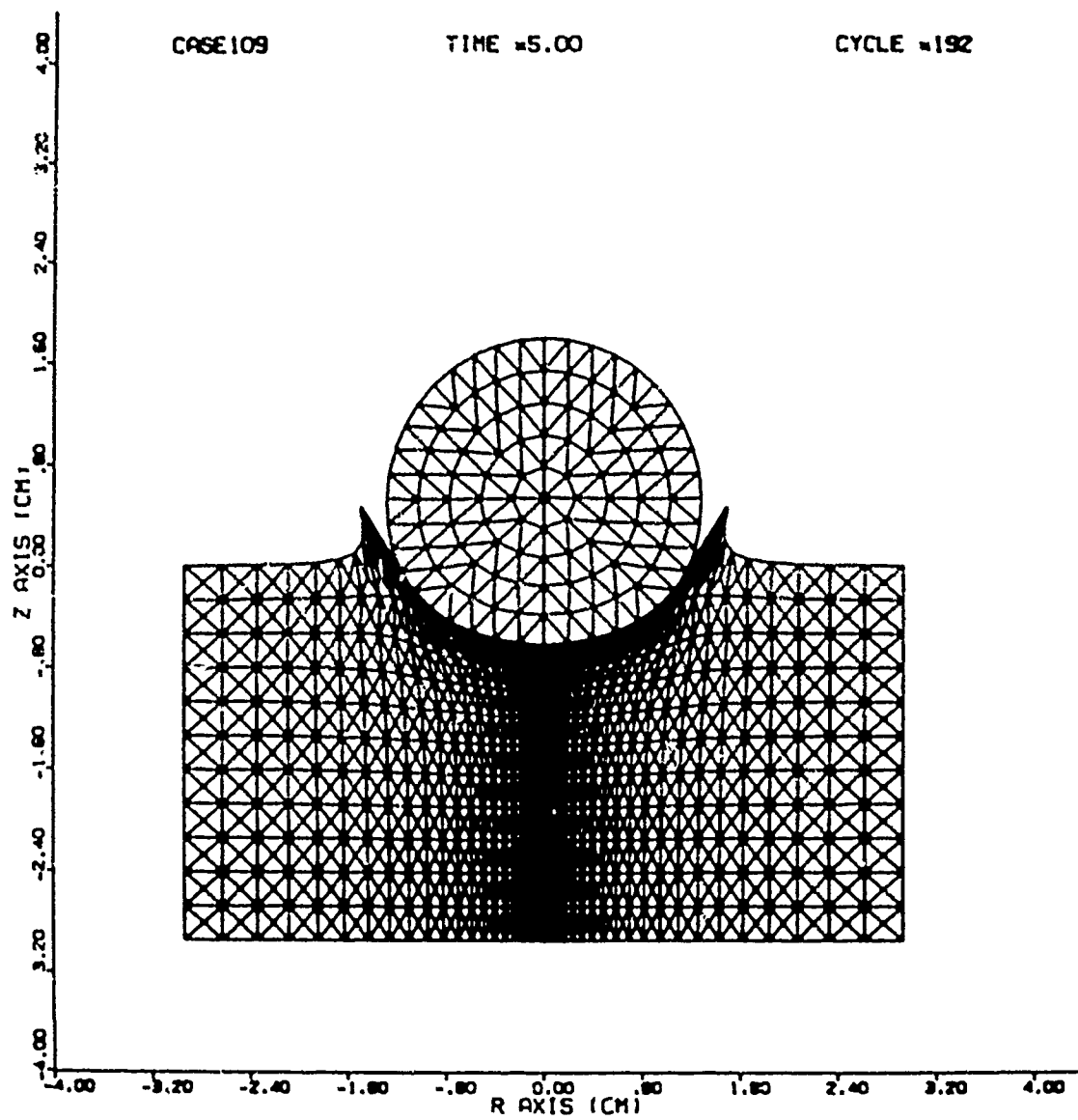
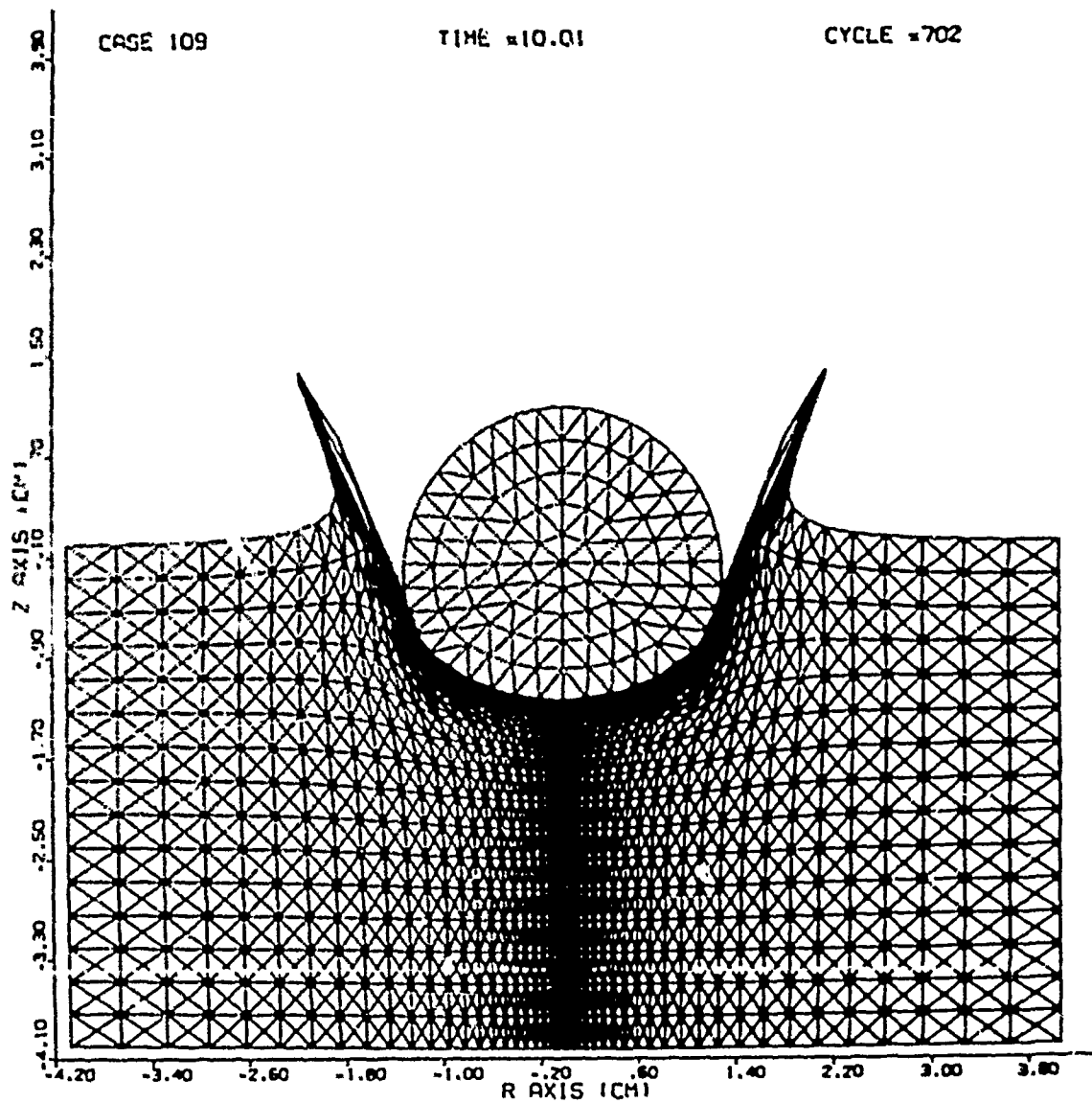Figure 23. Deformation of Sphere/Plate Impact, t = 5 μs, Triangles in Quadrilateral Elements.

38

Figure 24. Deformation Sphere/Plate Impact, t = 10μs, Triangles in Quadrilateral Elements.

the target, and the majority of the pressure fields in the target are located
in very small regions.


## IV. CONCLUSIONS


The elastic impact analyses demonstrate that close agreement between the
analytical (Skalak) and numerical solutions can be obtained provided a fine
grid with an aspect ratio of 1:1 is used. Coarse computational grids and high
aspect ratios prevent the numerical solution from capturing the high frequency
components.

For the effects of artificial viscosity upon wave propagation problems,
the linear term provides the additional dissipation required to obtain a
smooth, continuous solution, but it also tends to broaden the shock front.
The linear component should range between the values of 0.05 to 0.20 for the
best results. In most computer programs, the linear and quadratic components
are used in conjunction with each other in order to stabilize the effects of
excessive numerical ringing. The quadratic component is most effective when
the values range between 2.0 and 4.0 for the purpose of obtaining accurate
results.

In the cases studied, for the high velocity impact of a sphere into a
flat plate, the effects upon the failure of the elements, the deformation
behavior characteristics of the elements, and the pressure and strain fields
show that quadrilateral elements comprised of four triangles per quadrilateral
is the most reasonable representation of observed behavior in elastic-plastic
impact problems.

APPENDIX A


SPHERE/PLATE IMPACT
FAILED ELEMENT

Figure A1. Failed Elements, t = 5 µs, Case 107, IDIA = 1.

43

CASE 107/FAILURE          TIME =10.00                    CYCLE =448

Figure A2.   Failed Elements,  t = 10µs,  Case 107,  IDIA = 1.

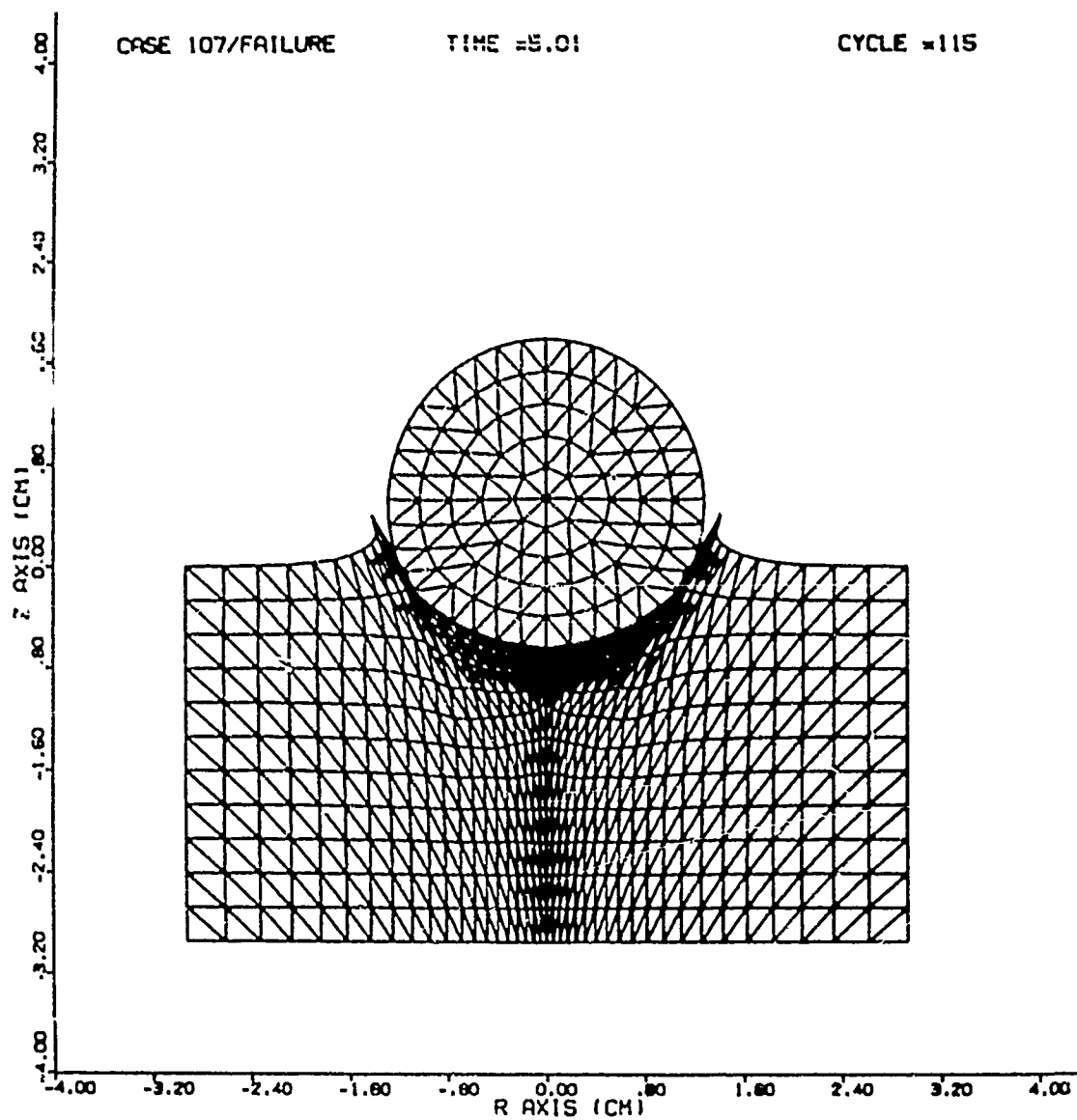CASE 108/FAILURE          TIME =5.01                    CYCLE =140
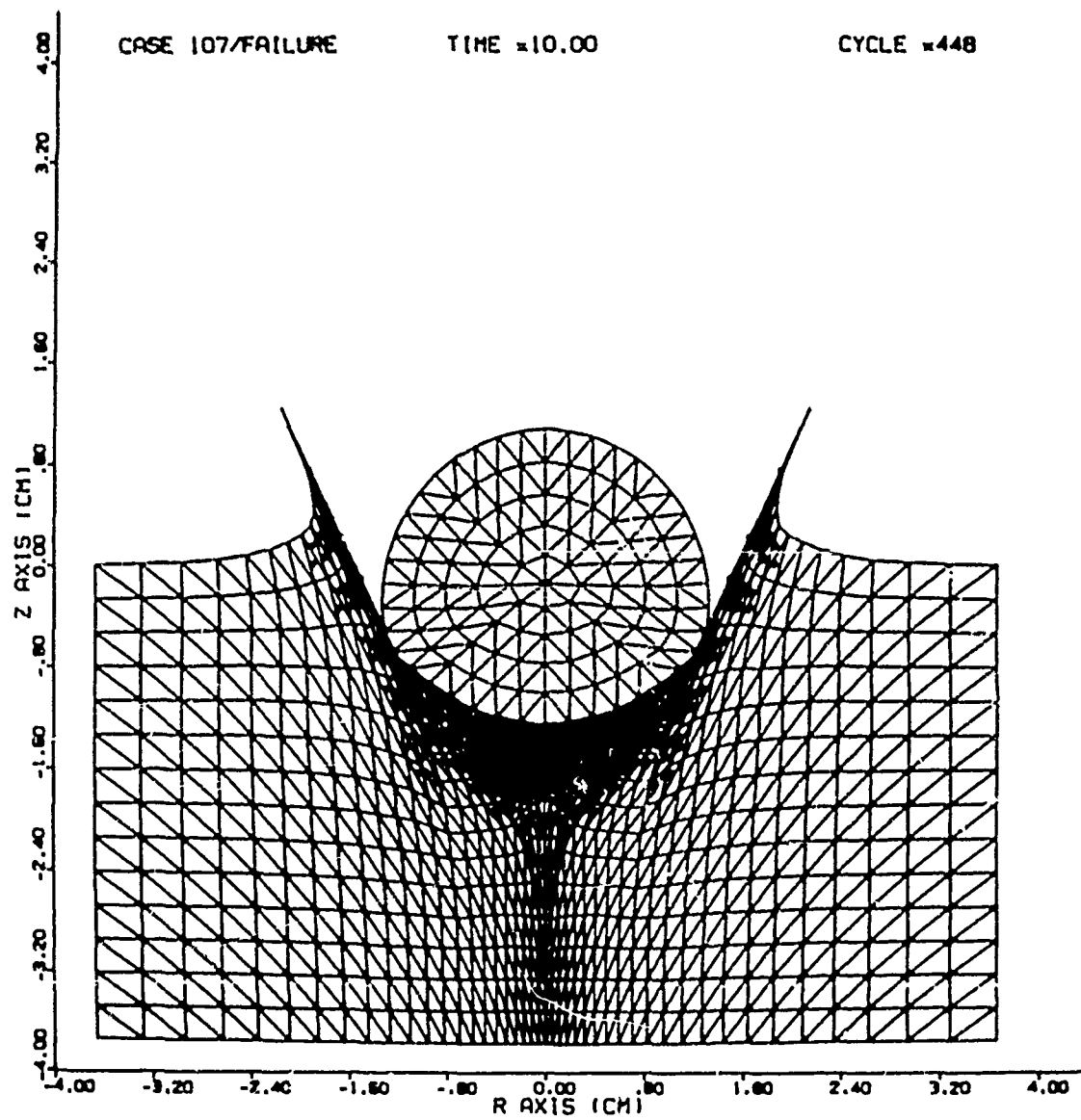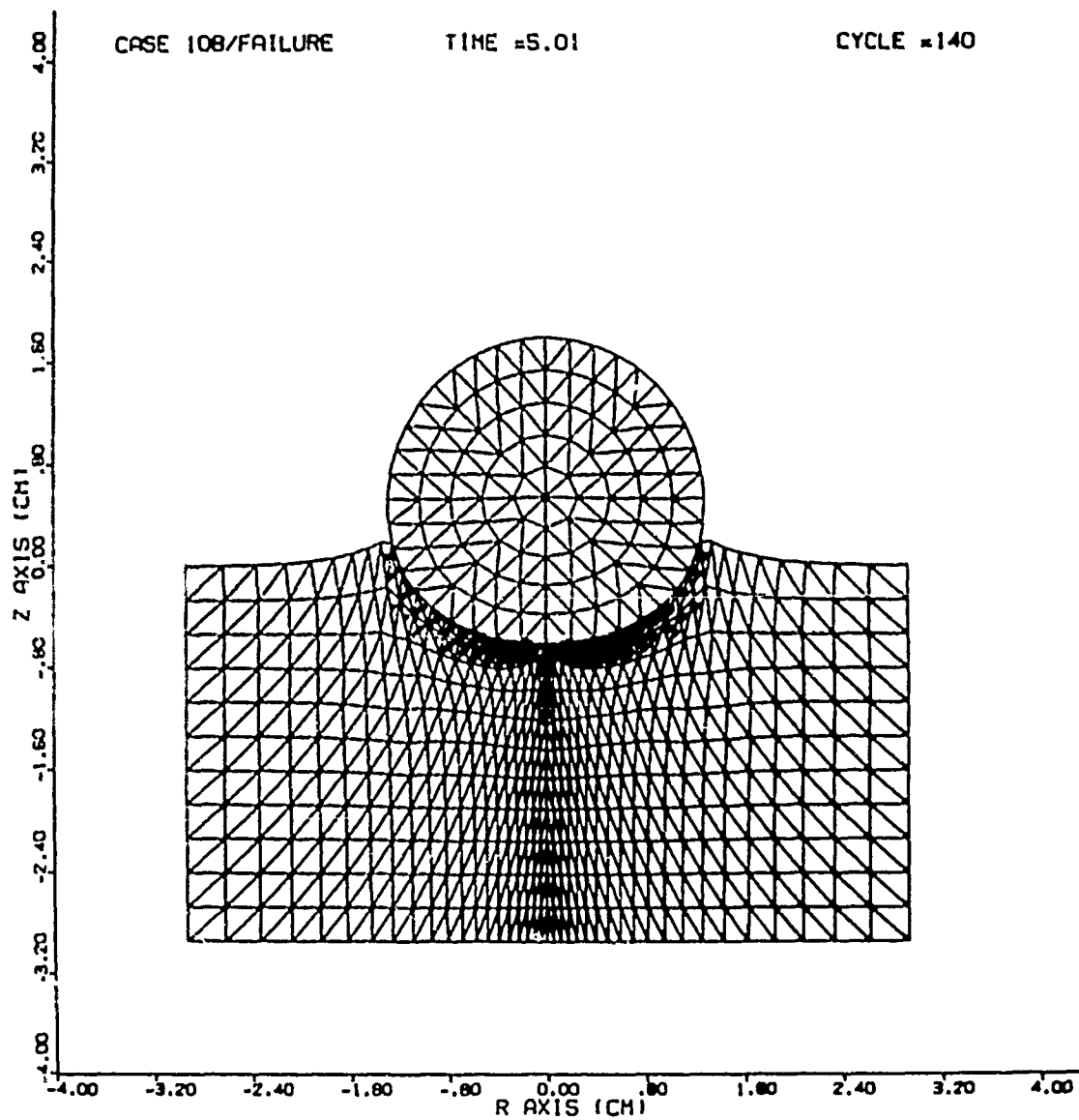
Figure A3.   Failed Elements, t = 5µs, Case 108, IDIA = 2.
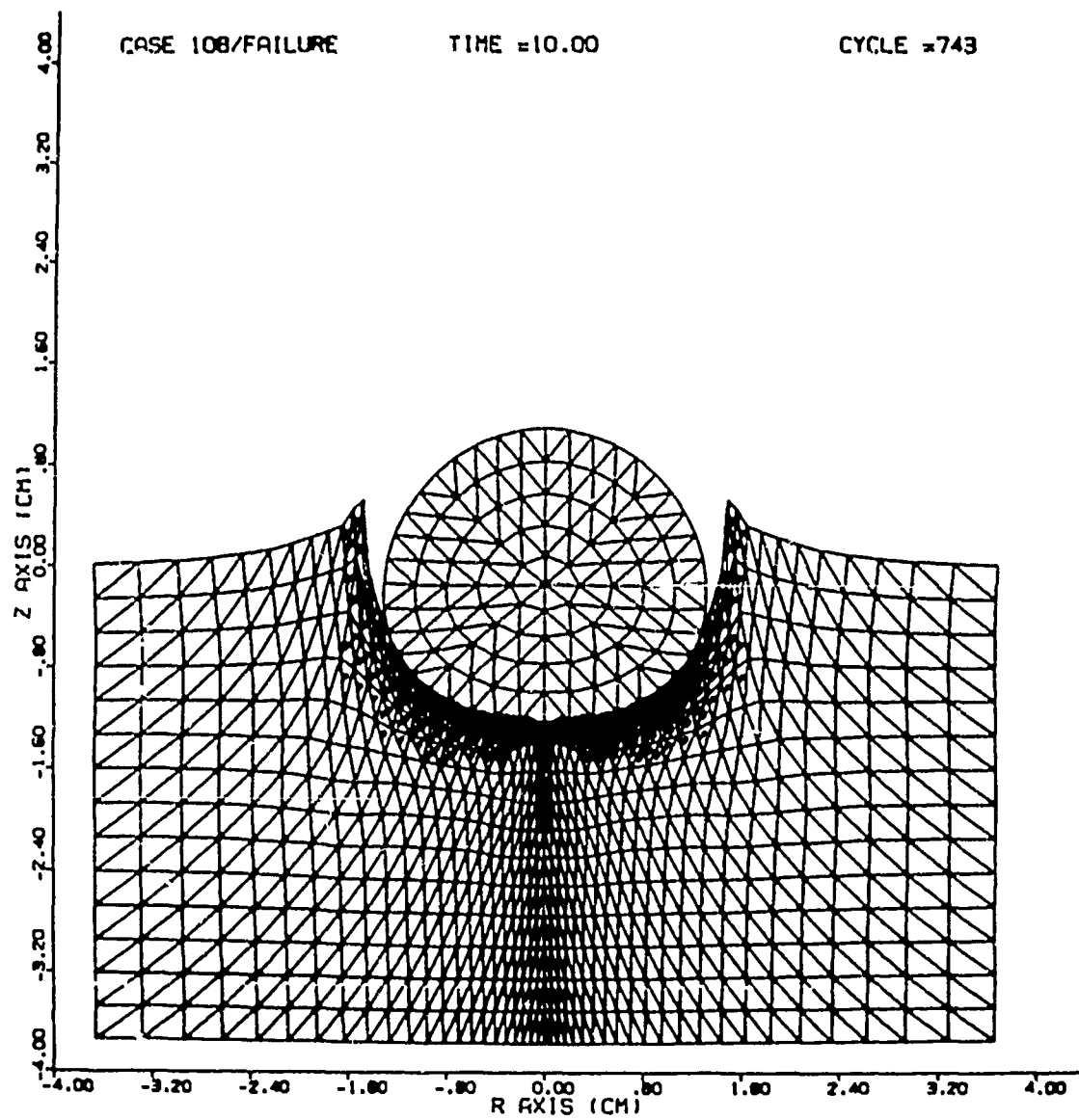
Figure A4.  Failed Elements, t = 10μs, Case 108, IDIA = 2.

46
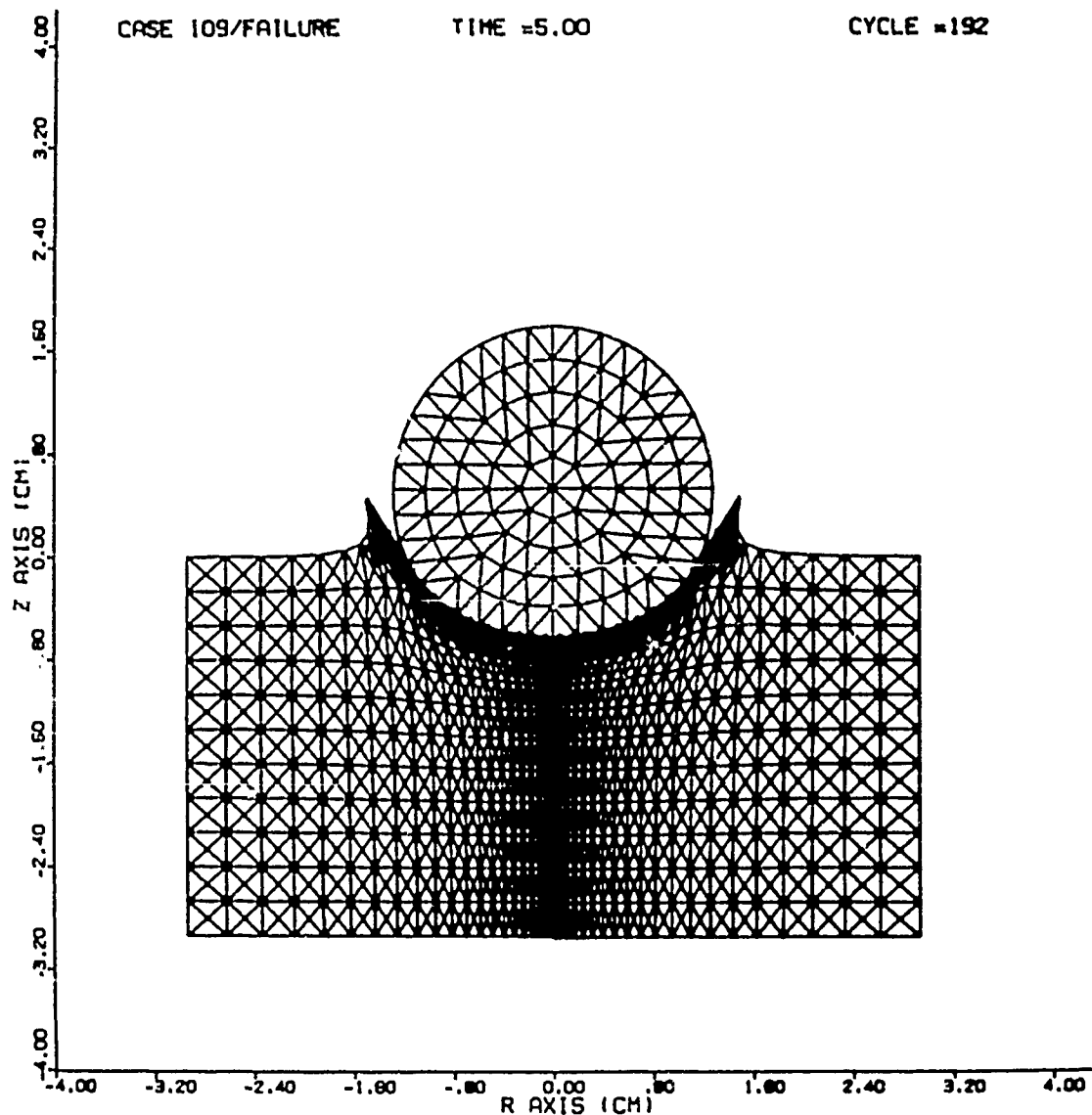
Figure A5.   Failed Elements, t = 5 μs, Case 109, Triangles in Quadrilateral Elements.

47
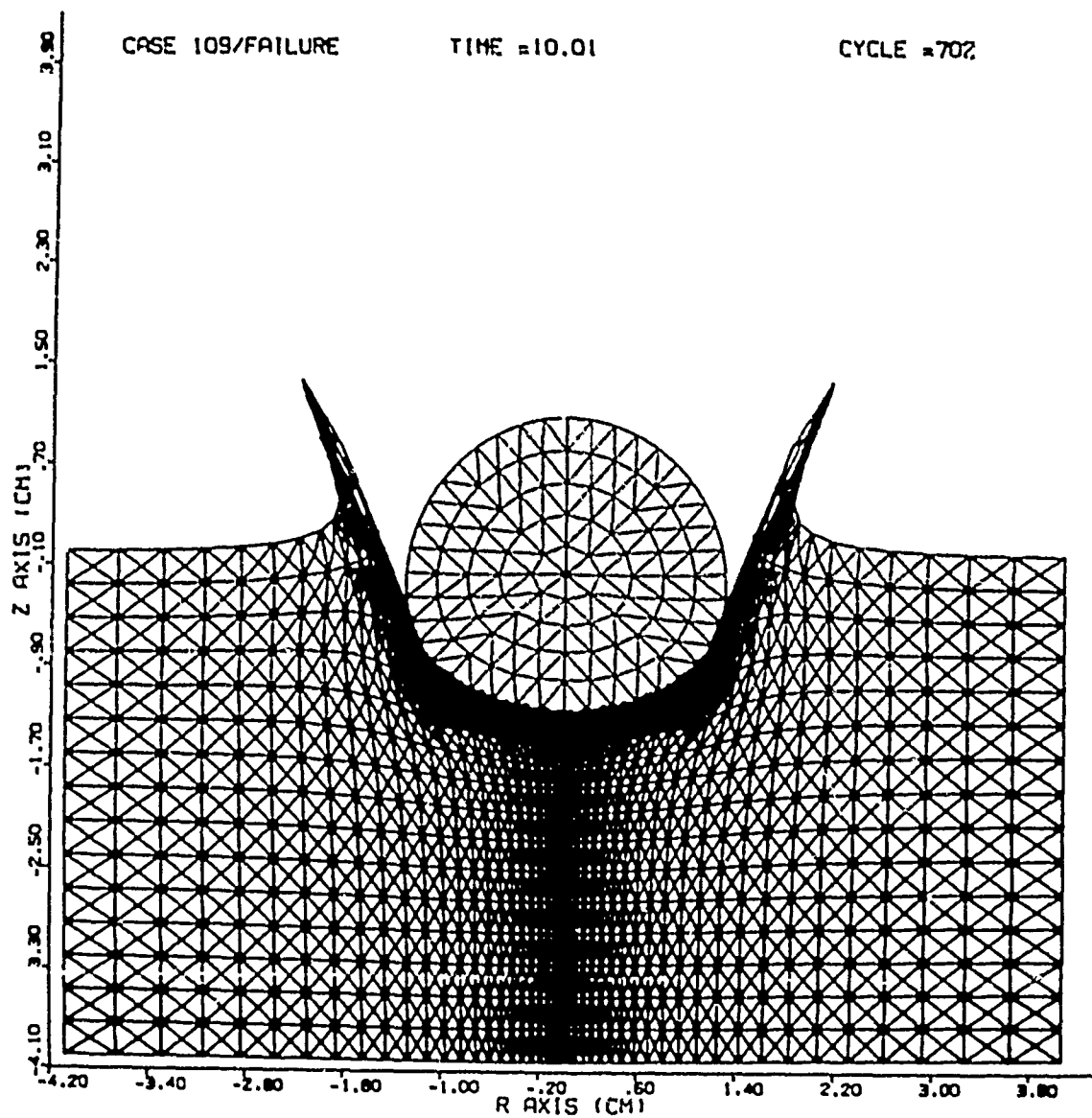
Figure A6.   Failed Elements, T= 10µs, Case 109, Triangles in Quadrilateral
             Elements.

48

APPENDIX B


SPHERE/PLATE IMPACT
STRAIN CONTOUR MAPS

49
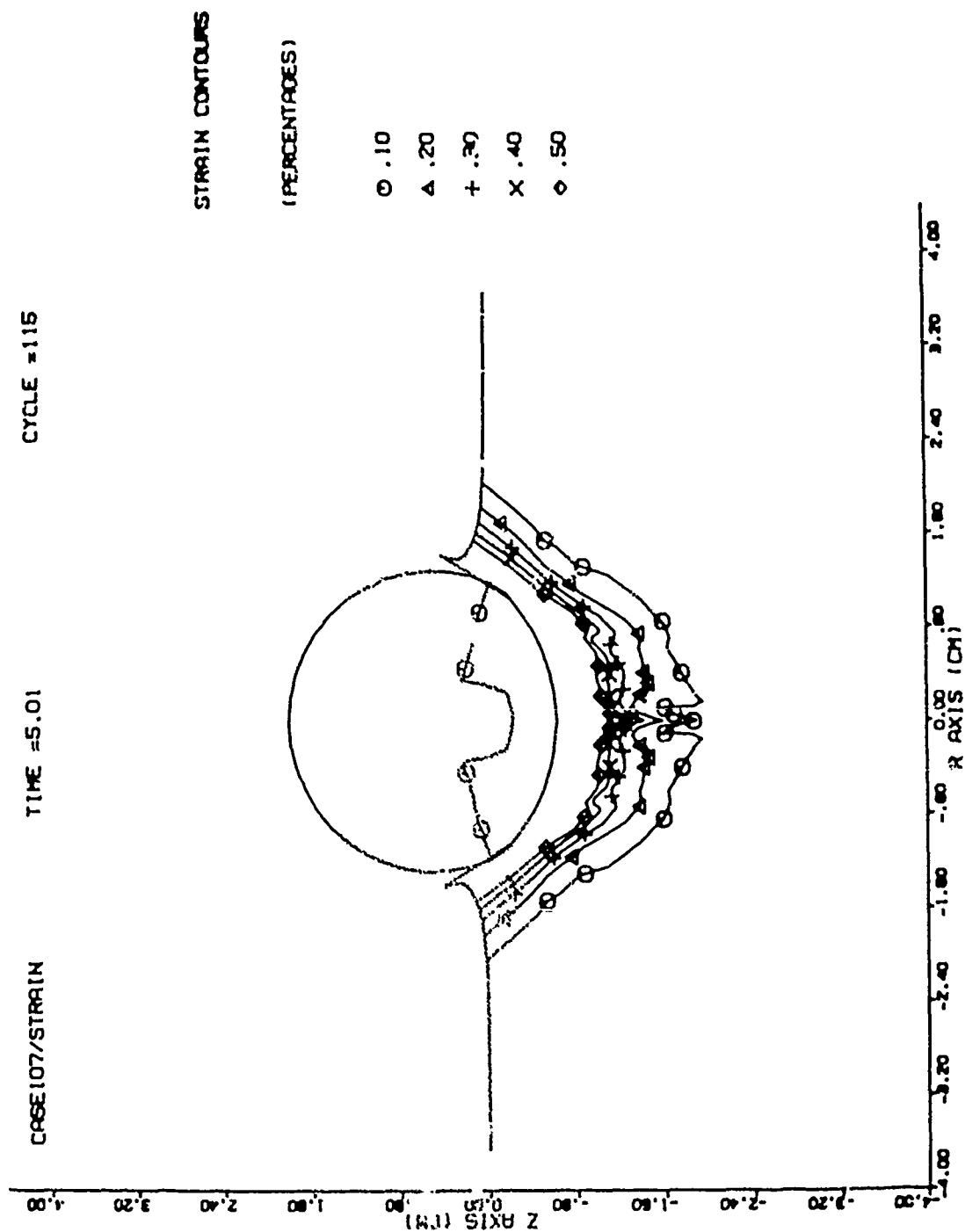
Figure B1. Strain Contour Map, t = 5μs, Case 107.

51
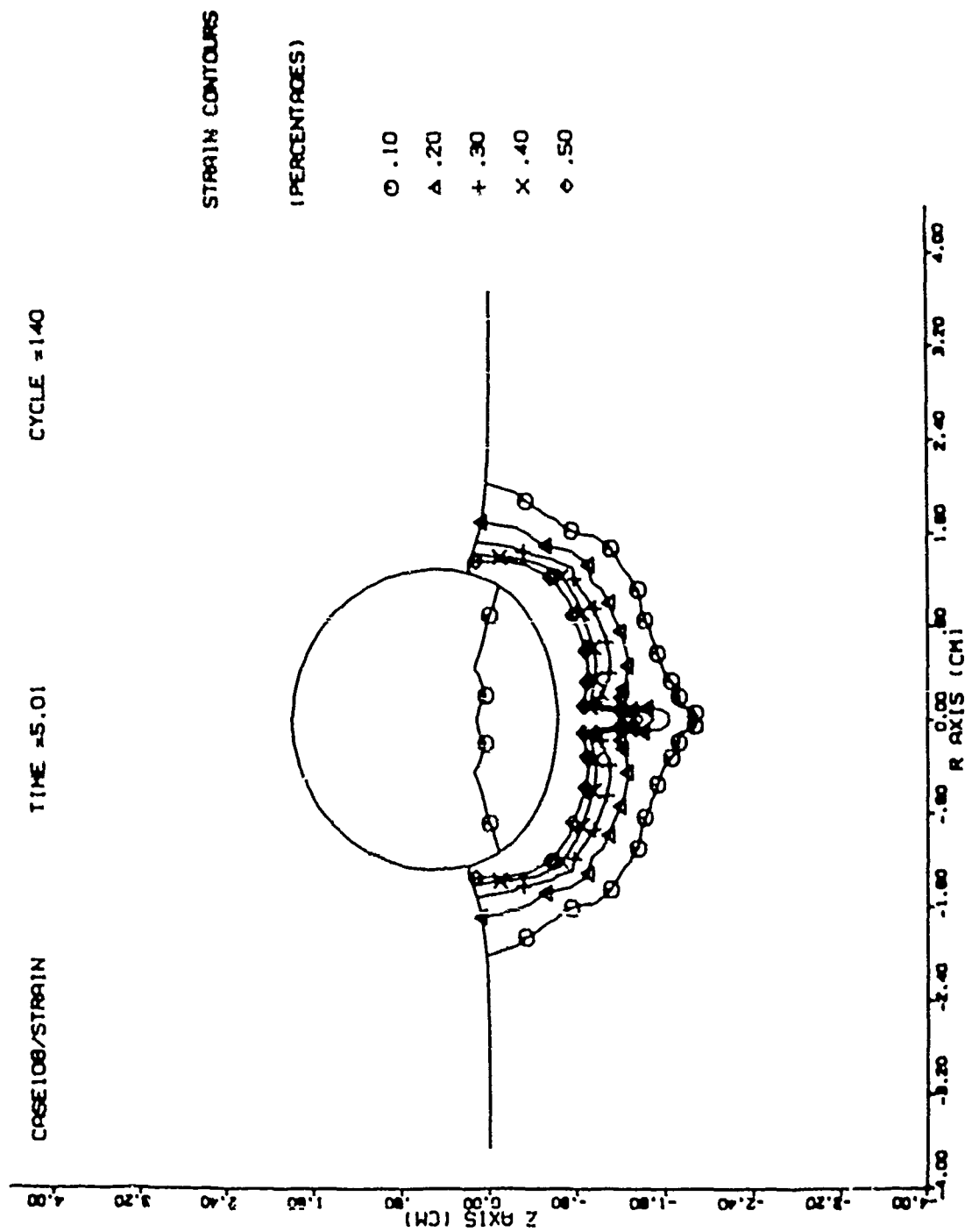
Figure B2. Strain Contour Map, t = 5μs, Case 103.

52
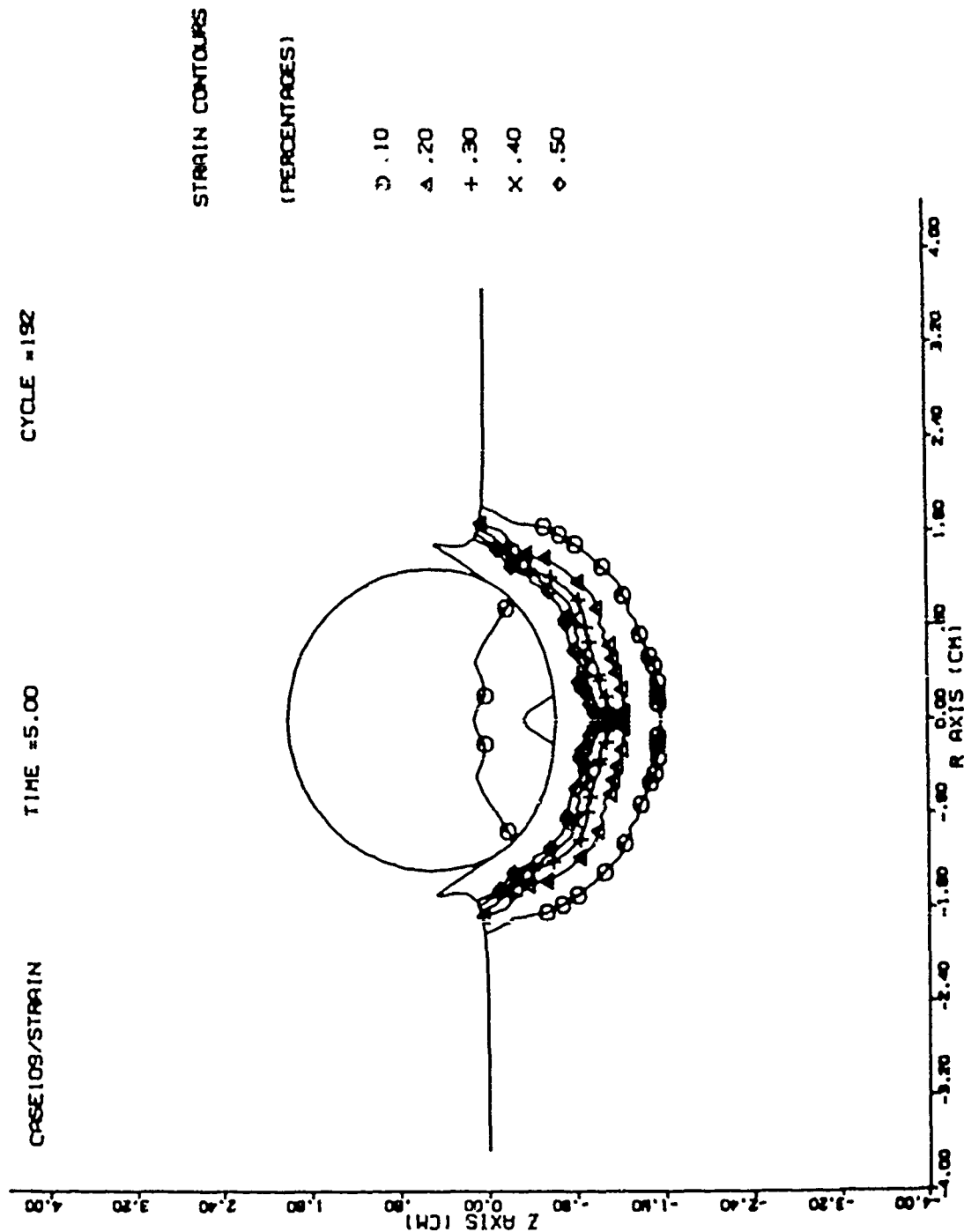
Figure E3. Strain Contour Map, t = 5μs, Case 109.
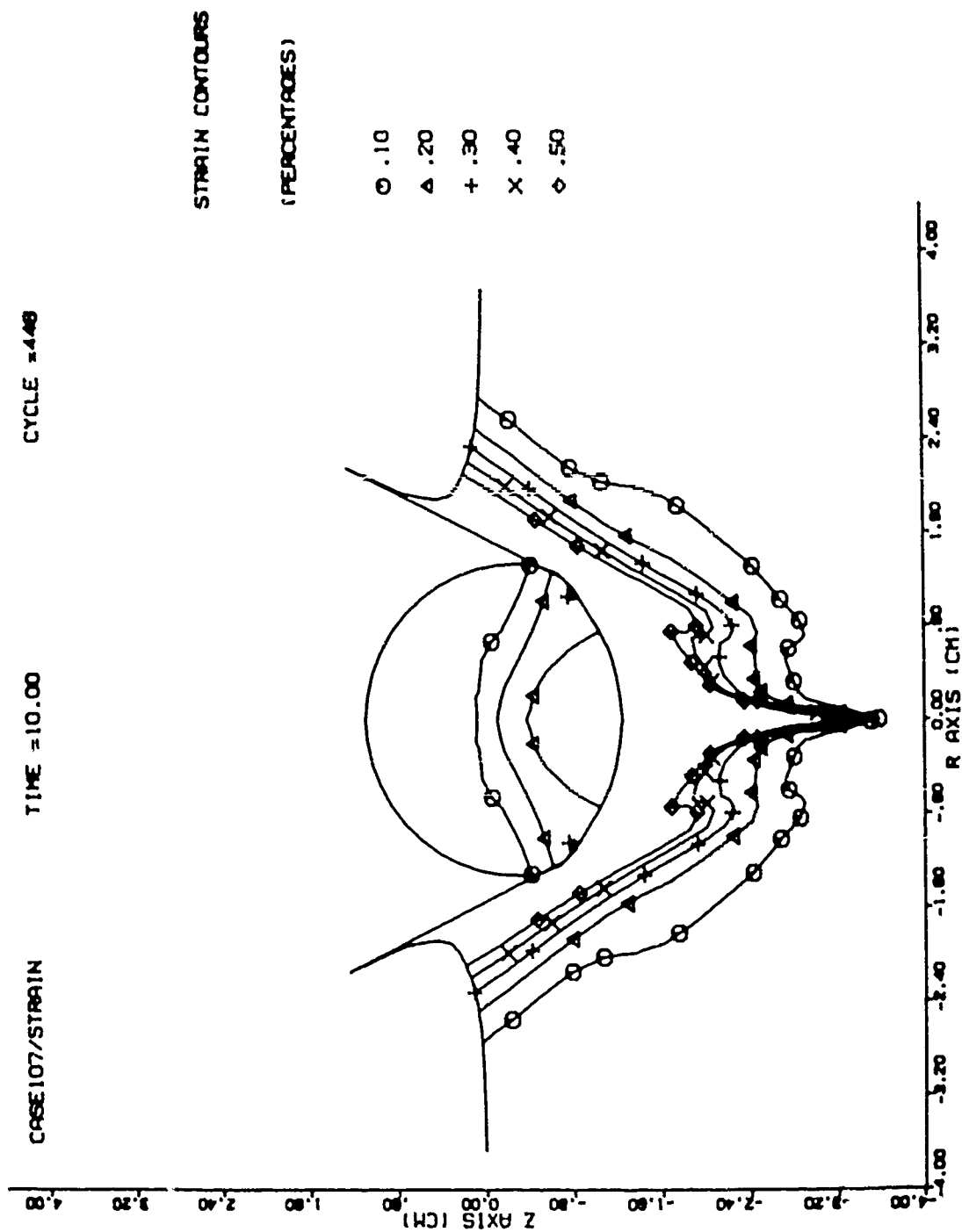
Figure B4. Strain Contour Map, t = 10μs, Case 107.

54

CASE108/STRAIN    TIME =10.00    CYCLE =743    STRAIN CONTOURS

(PERCENTAGES)

⊕ .10
▲ .20
+ .30
✕ .40
◇ .50
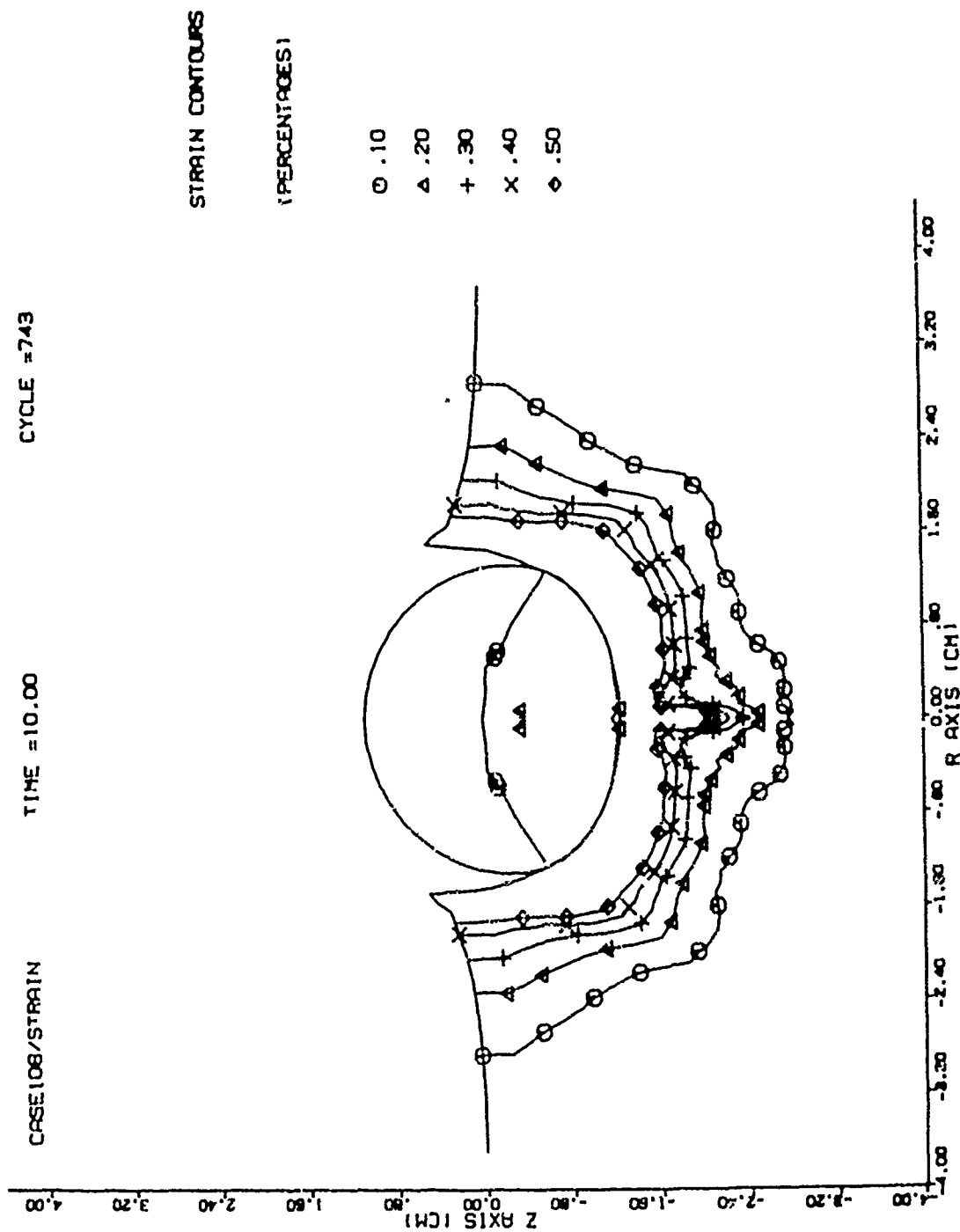
Figure B5. Strain Contour Map, t = 10μs, Case 108.

55
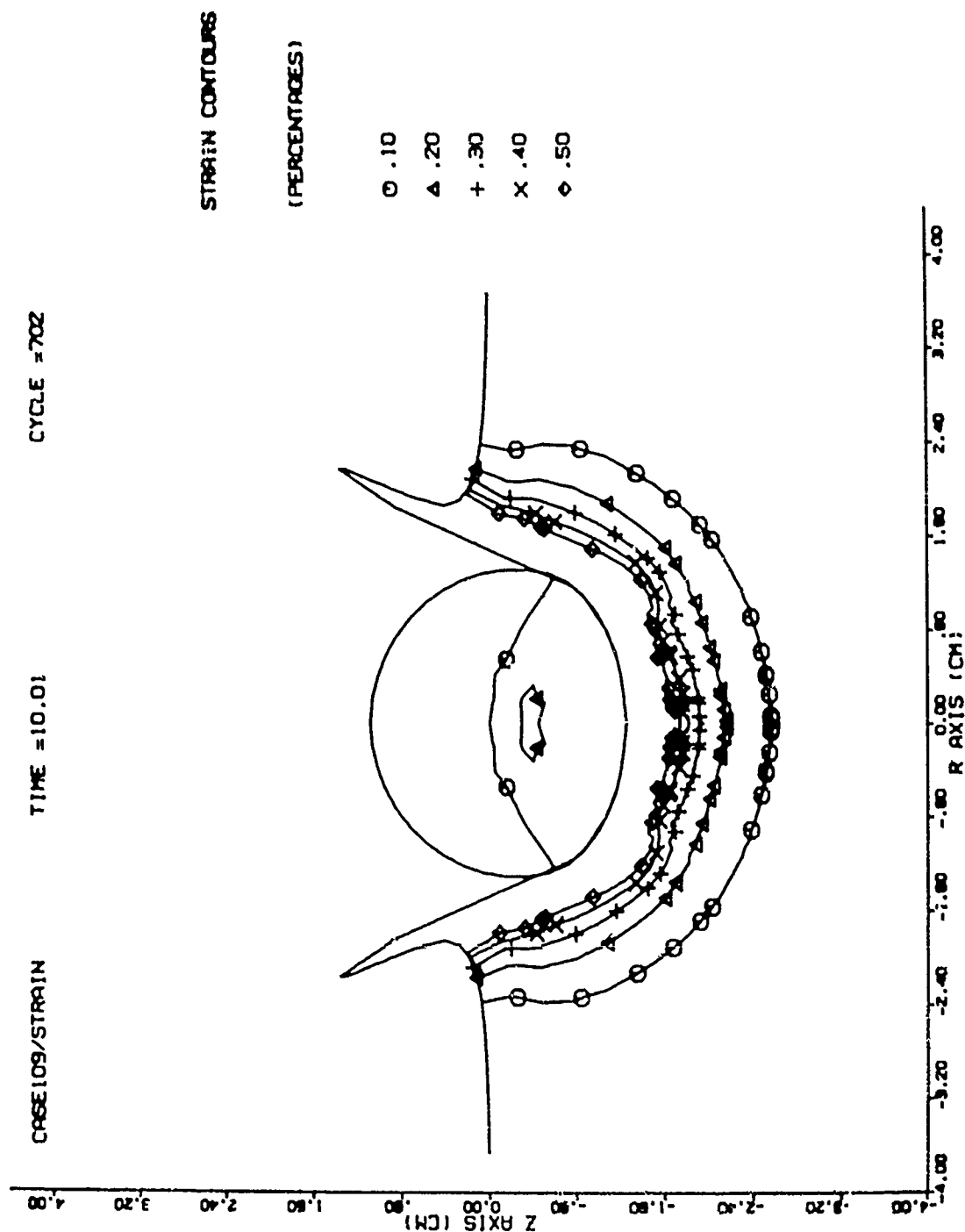
Figure B6. Strain Contour Map, t = 10μs, Case 109.

APPENDIX C


SPHERE/PLATE IMPACT
PRESSURE/NEGATIVE PRESSURE CONTOUR MAPS
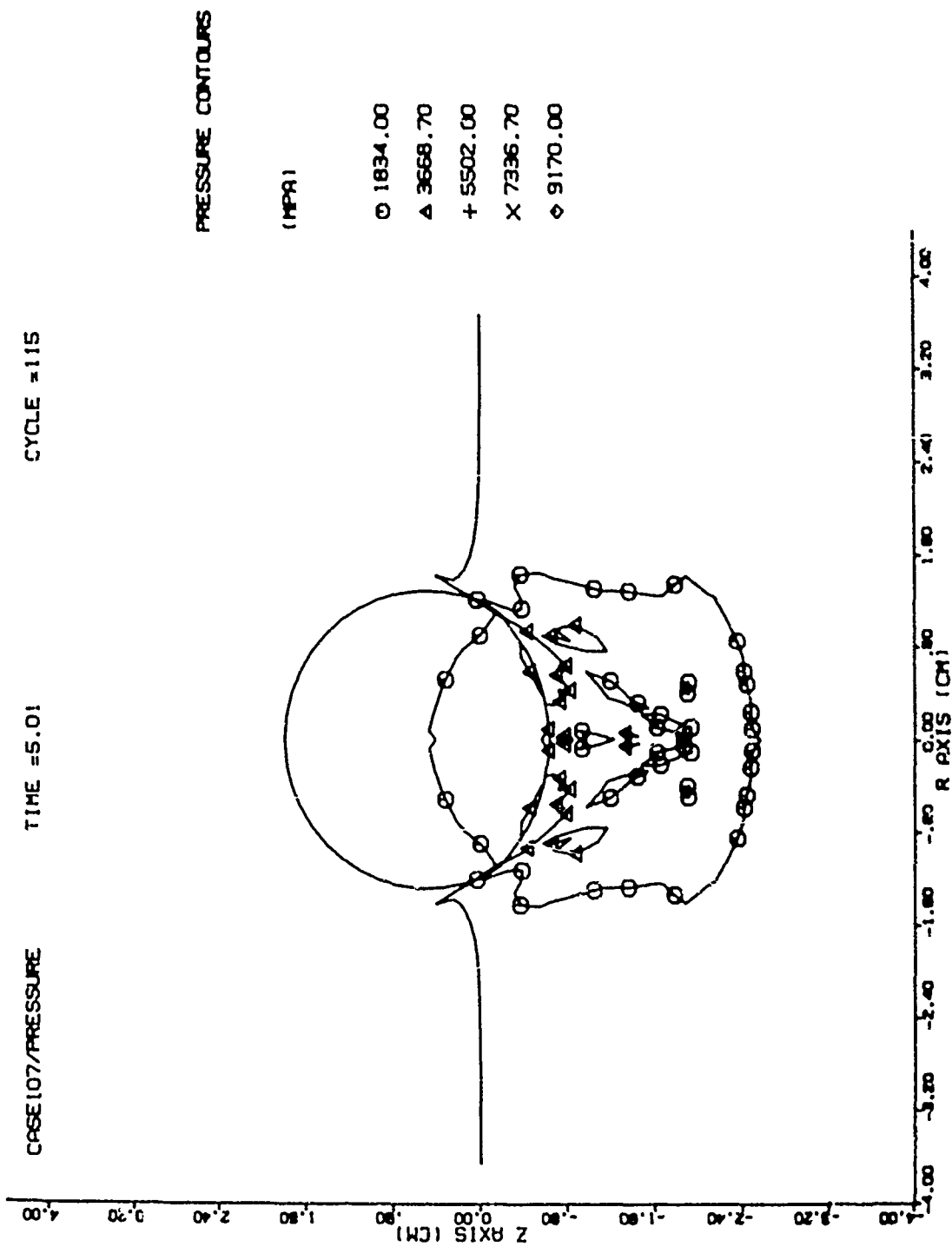
Figure C1. Pressure Contour Map, t = 5μs, Case 107.

59
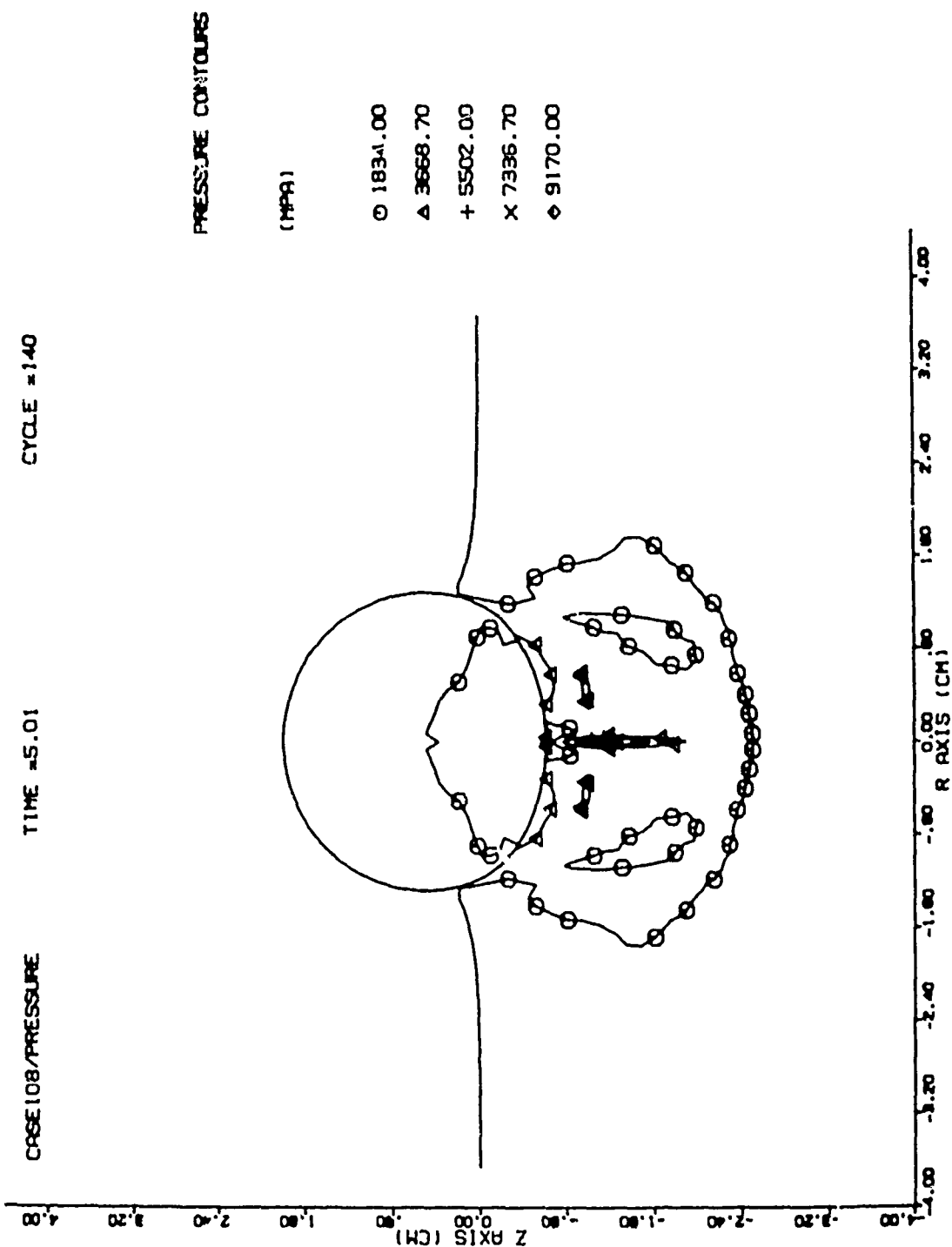
Figure C2. Pressure Contour Map, t = 5μs, Case 108.
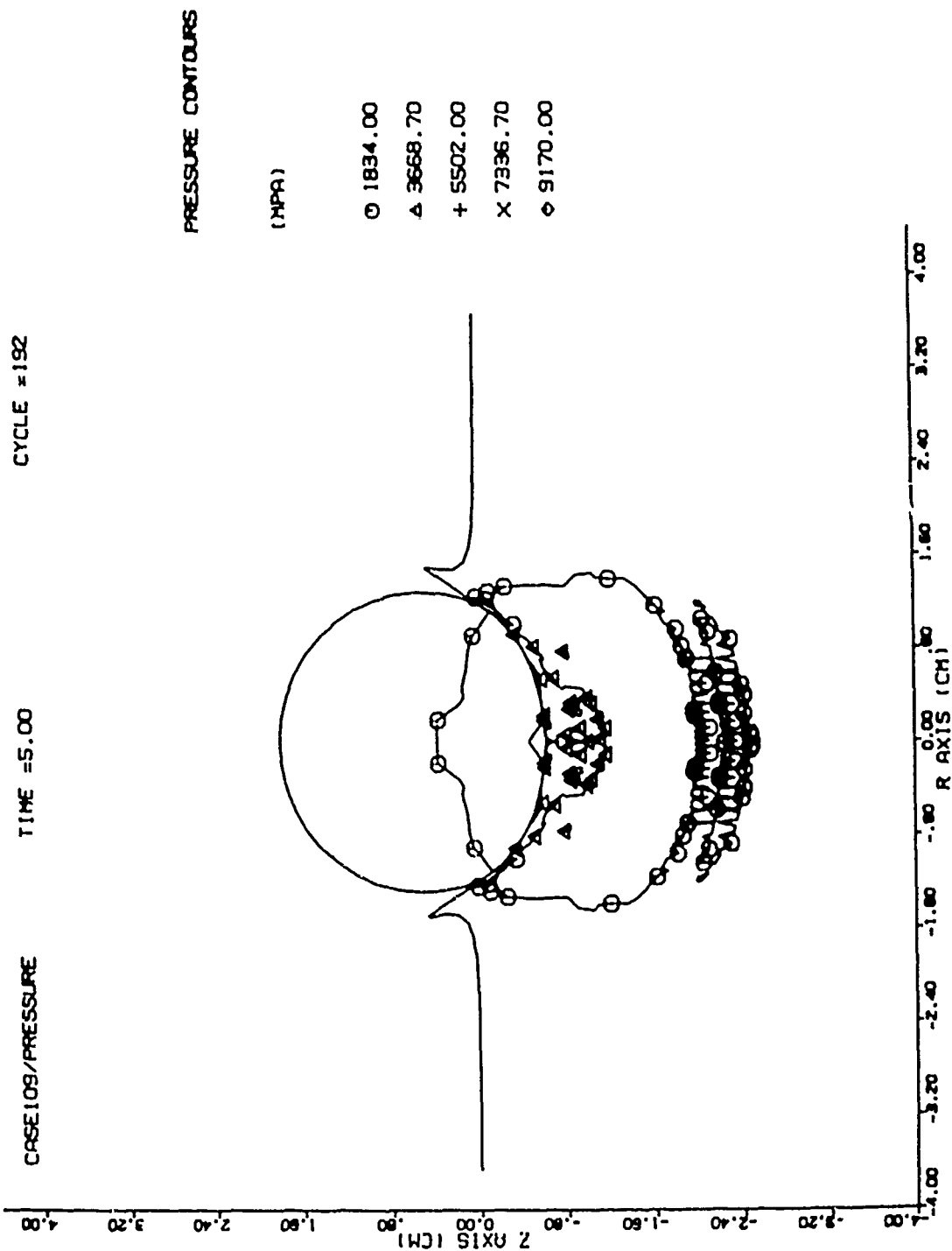
Figure C3. Pressure Contour Map, t = 5μs, Case 109.

61
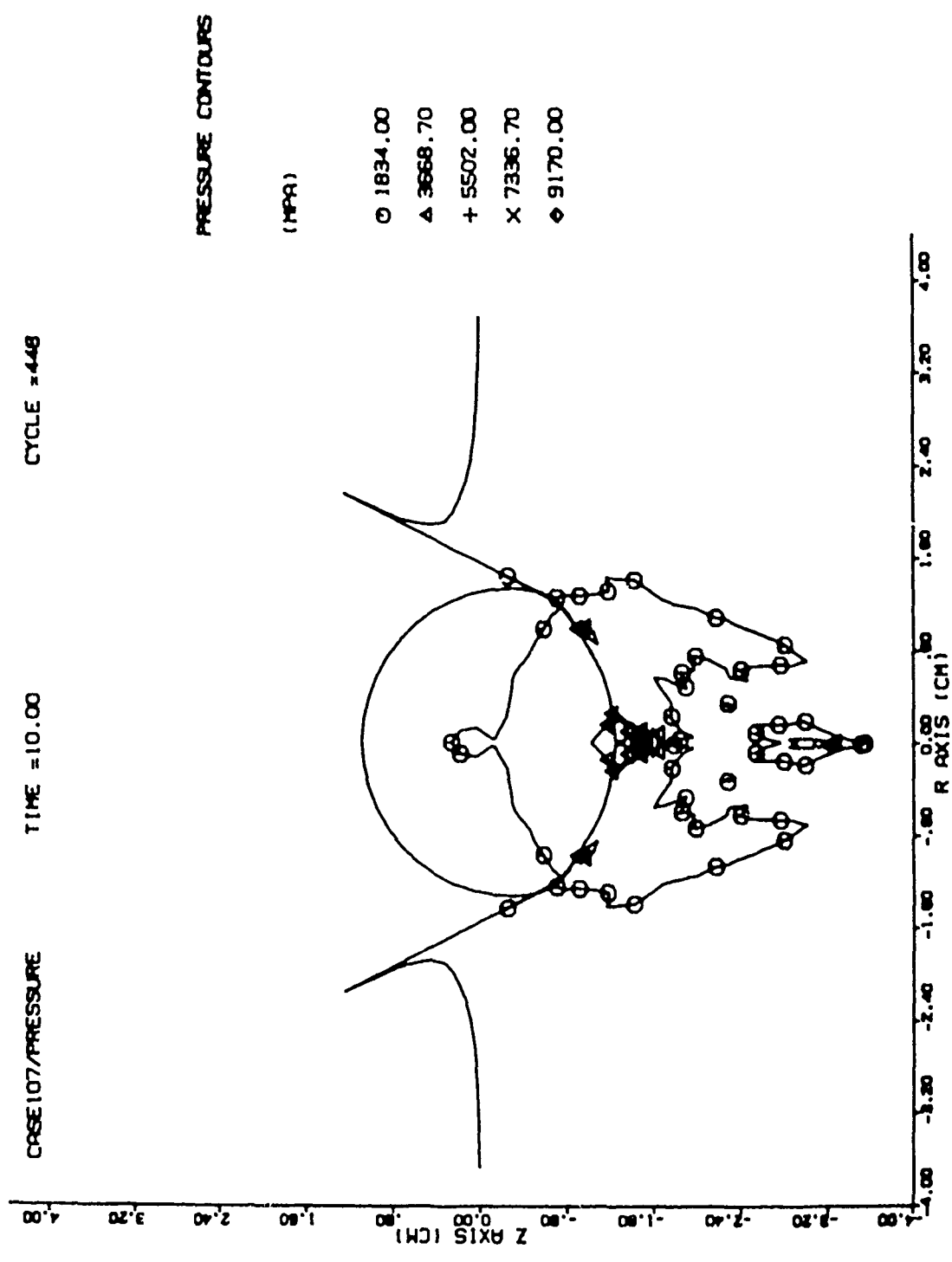
Figure C4. Pressure Contour Map, t = 10μs, Case 107.

Figure C5. Pressure Contour Map, $t = 10\mu s$, Case 108.

Figure C6. Pressure Contour Map, t = 10μs, Case 109.
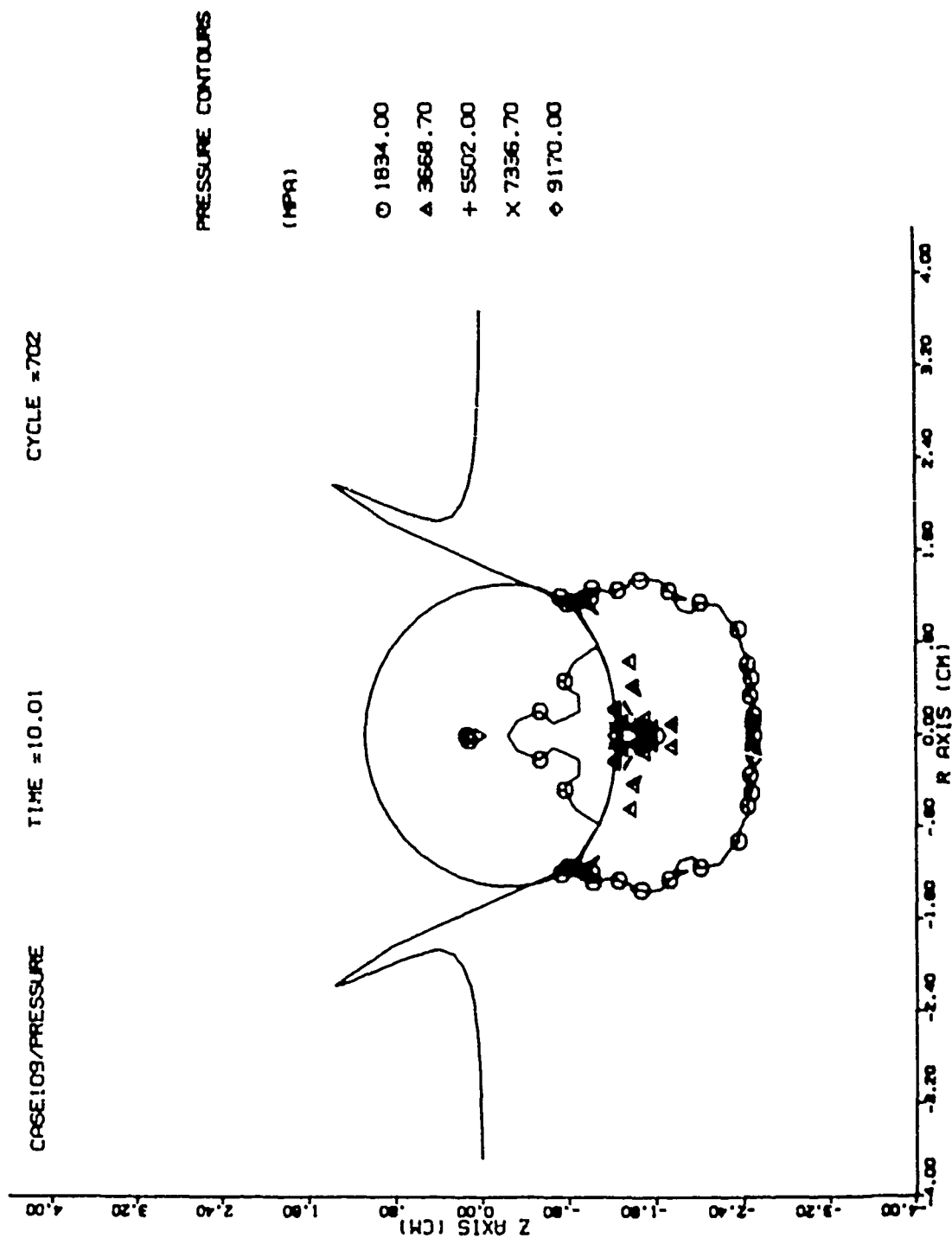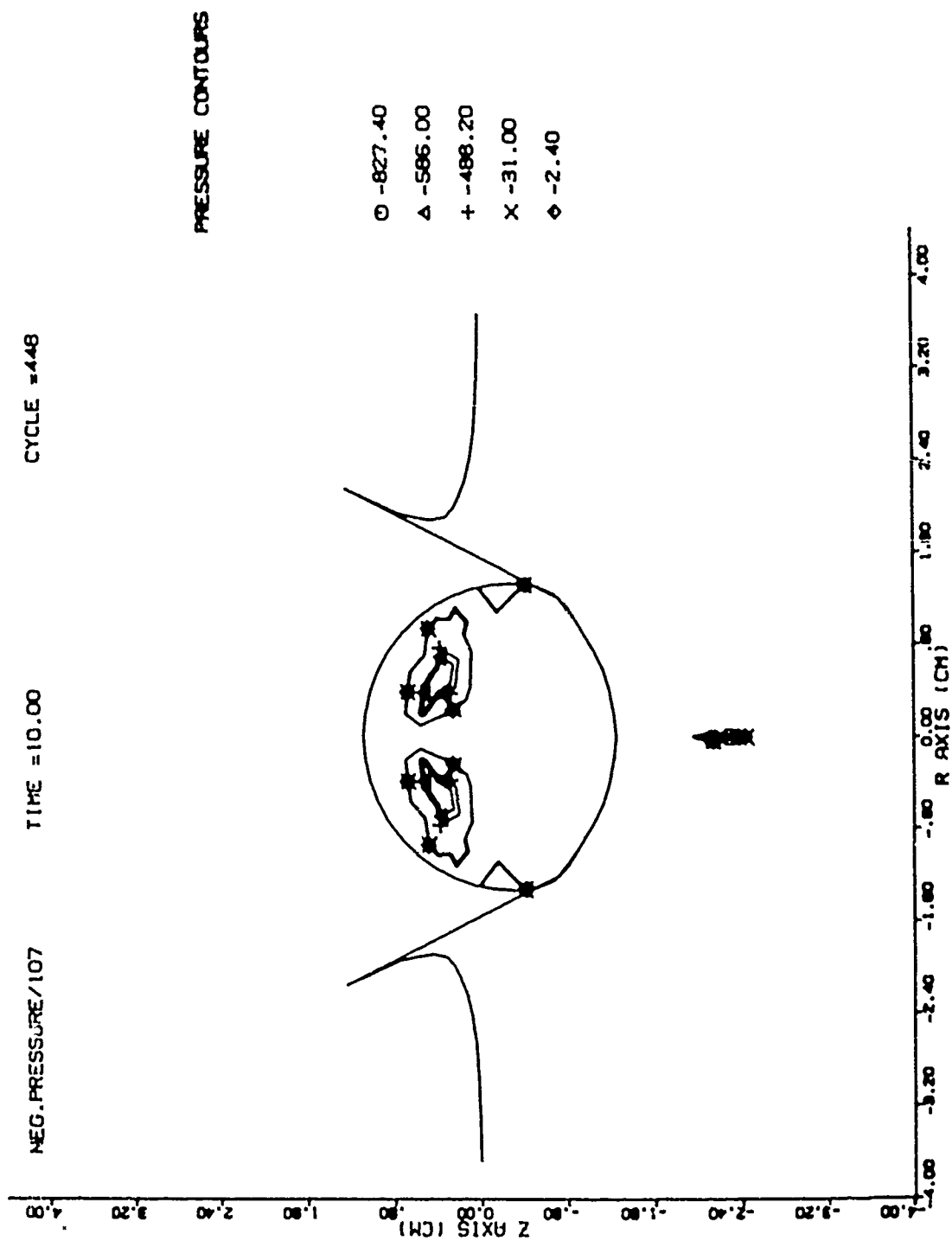
Figure C7. Negative Pressure Contour Map, t = 10μs, Case 107.

NEG.PRESSURE/107          TIME =10.00          CYCLE =448

PRESSURE CONTOURS

⊙ -827.40
△ -586.00
+ -488.20
× -31.00
◇ -2.40
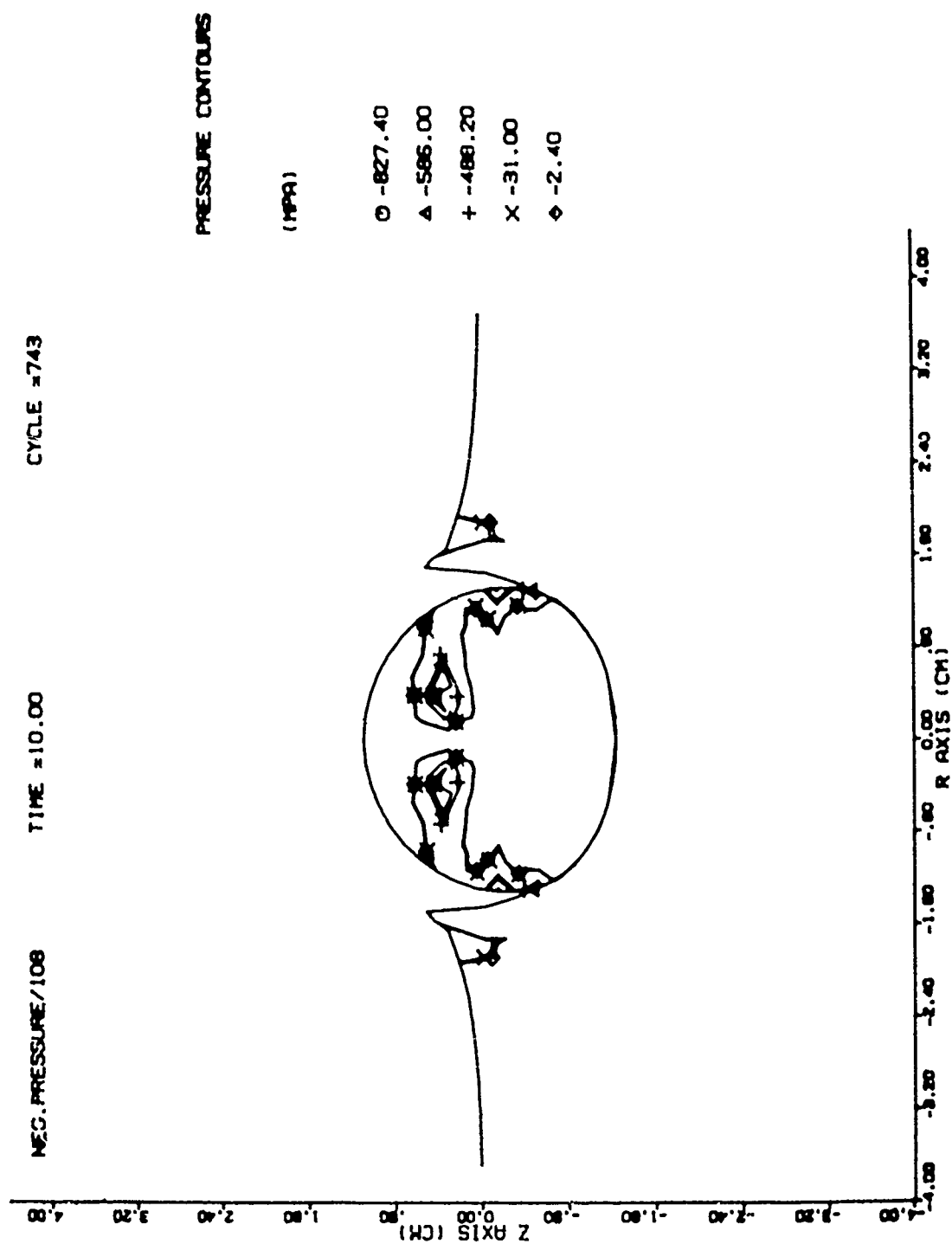
Figure C8. Negative Pressure Contour Map, $t = 10\mu s$, Case 108.
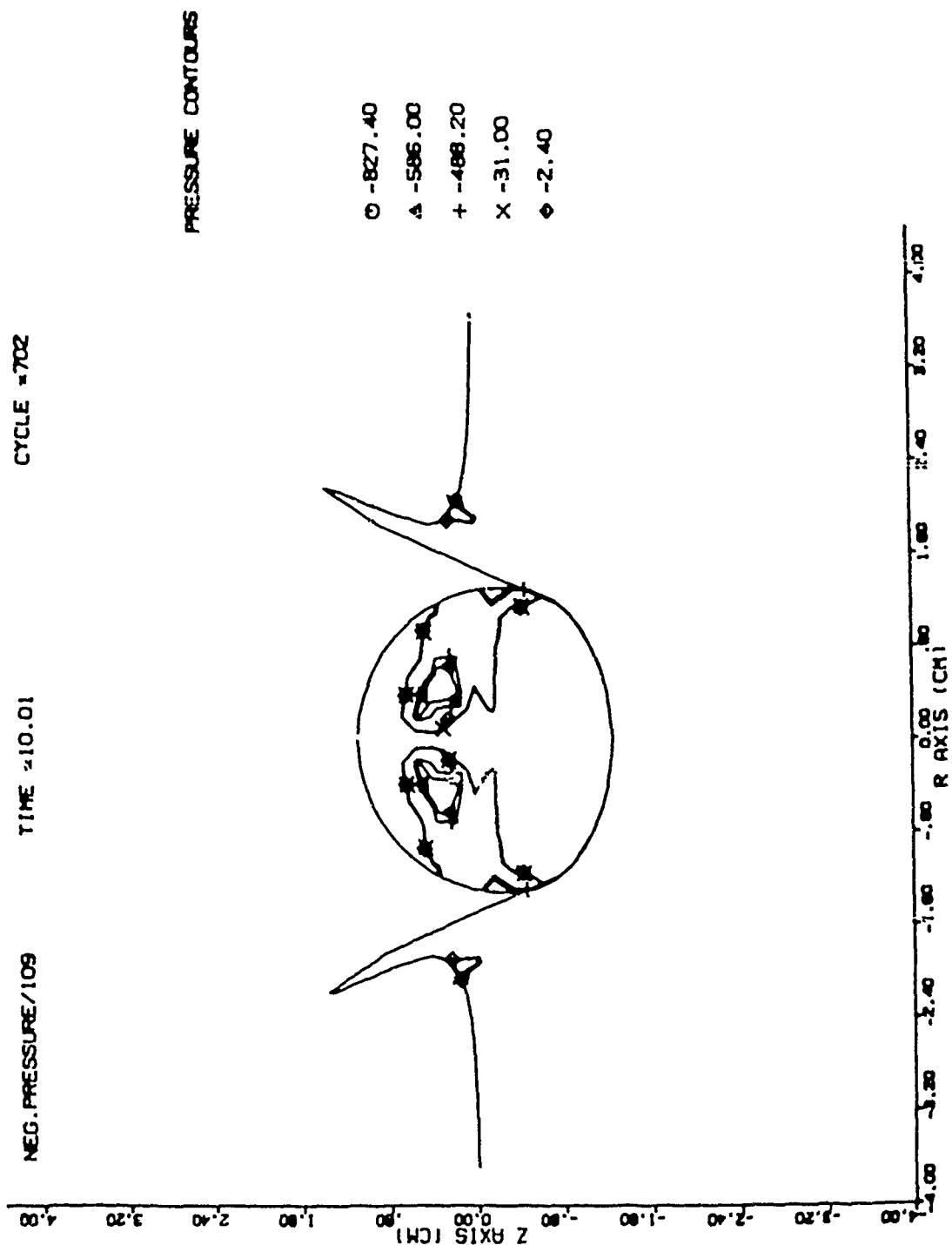
Figure C9. Negative Pressure Contour Map, $t = 10\mu s$, Case 109.

# DISTRIBUTION LIST

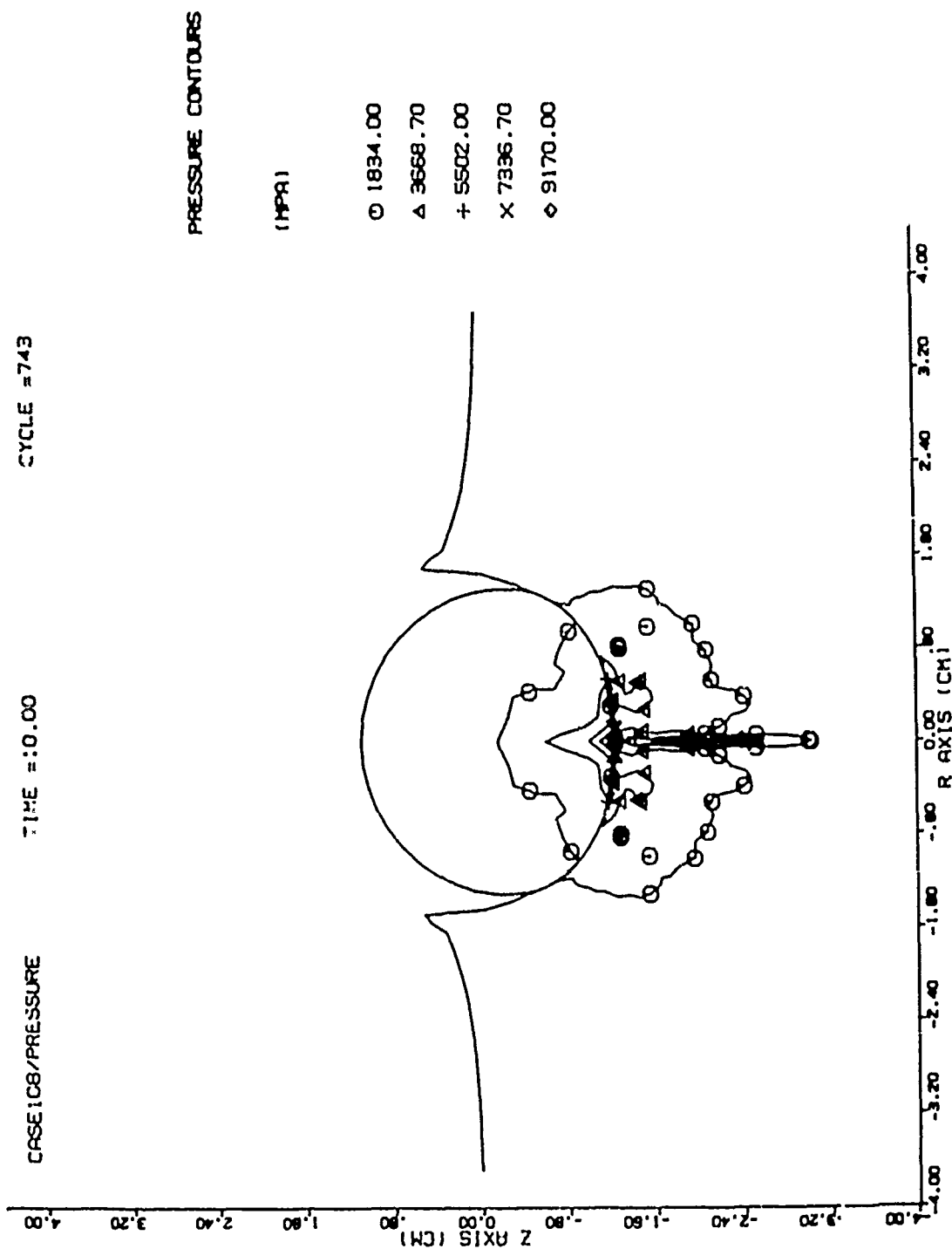| Copies | Organization | Copies | Organization |
|---|---|---|---|

12 Administrator
Defense Technical Info Center
ATTN: DTIC-DDA
Cameron Station
Alexandria, VA 22314

1 Director
Defense Advanced Research
  Projects Agency
ATTN: Tech Info
1400 Wilson Boulevard
Arlington, VA 22209

1 HQDA
DAMA-ART-M
Washington, DC 20310

1 Deputy Assistant Secretary
  of the Army (R&D)
Department of the Army
Washington, DC 20301

2 Commander
US Army BMD Advanced
  Technology Center
ATTN: BMDATC-M, Mr. S. Brockway
       BMDATC-RN, Mr. P. Boyd
PO Box 1500
Huntsville, AL 35807

1 HQDA (DAMA-ARP)
WASH DC 20310

1 HQDA (DAMA-MS)
WASH DC 20310

2 Commander
US Army Engineer Waterways
  Experiment Station
ATTN: Dr. P. Hadala
       Dr. B. Rohani
PO Box 631
Vicksburg, MS 39180

1 Commander
US Army Materiel Command
ATTN: AMCDRA-ST
5001 Eisenhower Avenue
Alexandria, VA 22333

10 Commander
Armament R&D Center
US Army AMCCOM
ATTN: SMCAR-TSS
      SMCAR-TDC
      SMCAR-TD, Dr. Weigle
      SMCAR-LC, Dr. J. Frasier
      SMCAR-SC, Dr. Gyorog
      SMCAR-LCF, G. Demitrack
      SMCAR-LCA,
        G. Randers-Pehrson
      SMCAR-SCS-M
        R. Kwatnoski
      SMCAR-LCU, E. Barrieres
      SMCAR-SCM, Dr. E. Bloore
Dover, NJ 07801

1 AFWL/SUL
Kirtland AFB, NM 87117

2 Director
Benet Weapons Laboratory
Armament R&D Center
US Army AMCCOM
ATTN: SMCAR-LCB-TL
        Dr. Joseph E. Flaherty
Watervliet, NY 12189

1 Commander
US Army Armament Materiel
  Readiness Command
ATTN: SMCAR-ESP-L,
Rock Island, IL 61299

1 Commander
US Army Aviation Research
  and Development Command
ATTN: AMSAV-E
4300 Goodfellow Blvd.
St. Louis, MO 63120

1 Director
US Army Air Mobility Research
  and Development Laboratory
Ames Research Center
Moffett Field, CA 94035

1 Commander
US Army Communications-
  Electronics Command
ATTN: AMSEL-ED
Fort Monmouth, NJ 07703

# DISTRIBUTION LIST

| Copies | Organization | Copies | Organization |
|---|---|---|---|

1 Commander
US Army Electronics Research
and Development Command
Technical Support Activity
ATTN: DELSD-L
Fort Monmouth, NJ 07703

1 Commander
US Army Missile Command
ATTN: AMSMI-RBL
Redstone Arsenal, AL 35898

3 Commander
US Army Tank-Automotive Command
ATTN: AMDTA-UL
AMSTA-TSL
V. H. Pagano
Warren, MI 48090

1 Commander
TARADCOM Tank-Automotive
Systems Laboratory
ATTN: T. Jean
Warren, MI 48090

6 Director
US Army Materials and
Mechanics Research Center
ATTN: AMXMR-T, Mr. J. Bluhm
Mr. J. Mescall
Dr. M. Lenoe
R. Shea
F. Quigley
AMXMR-ATL
Watertown, MA 02172

2 Commander
US Army Research Office
ATTN: Dr. E. Saibel
Dr. G. Mayer
PO Box 12211
Research Triangle Park
NC 27709-2211

1 Director
US Army TRADOC Systems
Analysis Activity
ATTN: ATAA-SL
White Sands Missile Range
NM 88002

1 Office of Naval Research
Department of the Navy
ATTN: Code ONR 439,
N. Perrone
800 North Quincy Street
Arlington, VA 22217

3 Commander
Naval Air Systems Command
ATTN: AIR-604
Washington, DC 20360

3 Commander
Naval Ordnance Systems Command
Washington, DC 20360

2 Commander
Naval Air Development
Center, Johnsville
Warminster, PA 18974

1 Commander
Naval Missile Center
Point Mugu, CA 93042

1 Commander
US Army Missile Command
ATTN: AMSMI-R
Redstone Arsenal, AL 35898

1 Commander & Director
David W. Taylor Naval Ship
Research & Development
Center
ATTN: Code 1740.4,
R. A. Gramm
Bethesda, MD 20084

1 Commander
US Army Missile Command
ATTN: AMSMI-YDL
Redstone Arsenal, AL 35898

70

# DISTRIBUTION LIST

| Copies | Organization | Copies | Organization |
|---|---|---|---|

1 Commander
Naval Surface Weapons Center
ATTN: Dr. W. G. Soper
Mr. N. Rupert
Code G35,
D. C. Peterson
Dahlgren, VA 22448

10 Commander
Naval Surface Weapons Center
ATTN: Dr. S. Fishman (2 cys)
Code R-13,
F. J. Zerilli
K. Kim
E. T. Toton
M. J. Frankel
Code U-11, J. R. Renzi
R. S. Gross
Code K-22, F. Stecher
J. Etheridge
Silver Spring, MD 20910

3 Commander
Naval Weapons Center
ATTN: Code 31804,
Mr. M. Smith
Code 326, Mr. P. Cordle
Code 3261,
Mr. T. Zulkoski
China Lake, CA 93555

6 Commander
Naval Weapons Center
ATTN: Code 3181, John Morrow
Code 3261,
Mr. C. Johnson
Code 3171,
Mr. B. Galloway
Code 3831,
Mr. M. Backman
Mr. R.E. VanDevender
Dr. O. E. R. Heimdahl
China Lake, CA 93555

2 Director
Naval Research Laboratory
ATTN: Dr. C. Sanday
Dr. H. Pusey
Washington, DC 20375

2 Superintendent
Naval Postgraduate School
ATTN: Dir of Lib
Dr. R. Ball
Monterey, CA 93940

3 Long Beach Naval Shipyard
ATTN: R. Kessler
T. Eto
R. Fernandez
Long Beach, CA 90822

1 HQ USAF/SAMI
Washington, DC 20330

1 AFIS/INOT
Washington, DC 20330

10 ADTC/DLJW (LT K. Ols)
Eglin AFB, FL 32542

10 ADTC/DLYV (Mr. J. Collins)
Eglin AFB, FL 32542

1 AFATL/DLYV
Eglin AFB, FL 32542

1 AFATL/DLODL
Eglin AFB, FL 32542-5000

1 AFATL/CC
Eglin AFB, FL 32542

1 AFATL/DLODR
Eglin AFB, FL 32542

1 HQ PACAF/DOOQ
Hickam AFB, HI 96853

1 HQ PACAF/OA
Hickam AFB, HI 96853

1 OOALC/MMWMC
Hill AFB, UT 84406

1 HQ TAC/DRA
Langley AFB, VA 23665

# DISTRIBUTION LIST

| Copies | Organization | Copies | Organization |
|---|---|---|---|

1 AUL-LSE 71-249
Maxwell AFB, AL 36112

1 AFWAL/MLLN (Mr. T. Nicholas)
Wright-Patterson AFB, OH 45433

1 ASD/ENESS (S. Johns)
Wright-Patterson AFB, OH 45433

1 ASD/ENFEA
Wright-Patterson AFB, OH 45433

1 ASD/XRP
Wright-Patterson AFB, OH 45433

1 HQUSAFE/DOQ
APO New York 09012

1 COMIPAC/I-32
Box 38
Camp H. I. Smith, HI 96861

10 Battelle Northwest
Laboratories
PO Box 999
ATTN: G. D. Marr
Richland, WA 99352

4 Lawrence Livermore Laboratory
PO Box 808
ATTN: Dr. R. Werne
Dr. J. O. Hallquist
Dr. M. L. Wilkins
Dr. G. Goudreau
Livermore, CA 94550

5 Los Alamos Scientific
Laboratory
PO Box 1663
ATTN: Dr. R. Karpp
Dr. J. Dienes
Dr. R. Keyser
Dr. E. Fugelso
Dr. D. E. Upham
Los Alamos, NM 87545

6 Sandia National Laboratory
ATTN: Dr. R. Woodfin
Dr. M. Sears
Dr. W. Herrmann
Dr. L. Bertholf
Dr. A. Chabai
Dr. C. B. Selleck
Albuquerque, NM 87115

1 Headquarters
National Aeronautics and
Space Administration
Washington, DC 20546

1 Jet Propulsion Laboratory
4800 Oak Grove Drive
ATTN: Dr. Ralph Chen
Pasadena, CA 91109

1 Director
National Aeronautics and
Space Administration
Langley Research Center
Langley Station
Hampton, VA 23365

1 US Geological Survey
2255 N. Gemini Drive
ATTN: Dr. D. Roddy
Flagstaff, AZ 86003

1 AAI Corporation
PO Box 6767
ATTN: R. L. Kachinski
Baltimore, MD 21204

1 Aerojet Ordnance Company
9236 East Hall Road
Downey, CA 90241

1 Aeronautical Research
Associates of
Princeton, Inc.
50 Washington Road
Princeton, NJ 08540

# DISTRIBUTION LIST

| Copies | Organization | Copies | Organization |
|---|---|---|---|

1 Aerospace Corporation
2350 E. El Segundo Blvd.
ATTN: Mr. L. Rubin
El Segundo, CA 90245

1 AVCO Systems Division
201 Lowell Street
ATTN: Dr. Reinecke
Wilmington, MA 01887

3 Battelle Columbus Laboratories
505 King Avenue
ATTN: Dr. G. T. Hahn
Dr. L. E. Hulbert
Dr. S. Sampath
Columbus, OH 43201

4 Boeing Company/Aerospace Division
ATTN: Mr. R. G. Blaisdell
(M.S. 40-25)
Dr. N. A. Armstrong,
C. J. Artura
(M.S. 8C-23)
Dr. B. J. Henderson
(M.S. 43-12)
P.O. Box 3707
Seattle, WA 98124

2 Brunswick Corporation
4300 Industrial Avenue
ATTN: P. S. Chang
R. Grover
Lincoln, NE 68504

1 Computer Code Consultants, Inc.
1680 Camino Redondo
ATTN: Dr. Wally Johnson
Los Alamos, NM 87544

1 Dresser Center
PO Box 1407
ATTN: Dr. M. S. Chawla
Houston, TX 77001

1 Effects Technology, Inc.
5383 Hollister Avenue
Santa Barbara, CA 93111

1 Electric Power Research
Institute
PO Box 10412
ATTN: Dr. George Sliter
Palo Alto, CA 94303

1 FMC Corporation
Ordnance Engineering Division
San Jose, CA 95114

1 Ford Aerospace and
Communications Corporation
Ford Road, PO Box A
ATTN: L. K. Goodwin
Newport Beach, CA 92663

1 General Dynamics
PO Box 2507
ATTN: J. H. Cuadros
Pomona, CA 91766

1 General Electric Company
Lakeside Avenue
ATTN: D. Graham, Rm 1311
Burlington, VT 05401

1 President
General Research Corporation
ATTN: Lib
McLean, VA 22101

1 Goodyear Aerospace Corporation
1210 Massilon Road
Akron, OH 44315

1 H. P. White Laboratory
3114 Scarboro Road
Street, MD 21154

5 Honeywell, Inc.
Government and Aerospace
Products Division
ATTN: Mr. J. Blackburn
Dr. G. Johnson
Mr. R. Simpson
Mr. K. H. Doeringsfeld
Dr. D. Vavrick
600 Second Street, NE
Hopkins, MN 55343

73

# DISTRIBUTION LIST

| Copies | Organization | Copies | Organization |
|---|---|---|---|

1    Hughes Aircraft Corporation
ATTN: Mr. W. Keppel
       MS M-5, Bldg 808
Tucson, AZ 85706

2    Kaman Sciences Corporation
1500 Garden of the Gods Road
ATTN: Dr. P. Snow
       Dr. D. Williams
Colorado Springs, CO 80907

1    Lockheed Palo Alto Research
     Laboratory
3251 Hanover Street
ATTN: Org 5230, Bldg 201
       Mr. R. Robertson
Palo Alto, CA 94394

1    Lockheed Missiles and Space
     Company
PO Box 504
ATTN: R. L. Williams
       Dept. 81-11, Bldg 154
Sunnyvale, CA 94086

1    Materials Research
     Laboratory, Inc.
1 Science Road
Glenwood, IL 60427

2    McDonnell-Douglas Astro-
     nautics Company
5301 Bolsa Avenue
ATTN: Dr. L. B. Greszczuk
       Dr. J. Wall
Huntington Beach, CA 92647

1    New Mexico Institute of
     Mining and Technology
ATTN: TERA Group
Socorro, NM 87801

1    Northrop Norair
3901 W. Broadway
ATTN: R. L. Ramkumar
Hawthorne, CA 90250

1    Nuclear Assurance Corporation
24 Executive Park West
ATTN: T. C. Thompson
Atlanta, GA 30245

2    Orlando Technology, Inc.
PO Box 855
ATTN: Mr. J. Osborn
       Mr. D. Matuska
Shalimar, FL 32579

1    Commandant
US Army Infantry School
ATTN: ATSH-CD-CSO-OR
Fort Benning, GA 31905

1    Rockwell International
Missile Systems Division
ATTN: A. R. Glaser
4300 E. Fifth Avenue
Columbus, OH 43216

3    Schumberger Well Services
Perforating Center
ATTN: J. E. Brooks
       J. Brookman
       Dr. C. Aseltine
PO Box A
Rosharon, TX 77543

1    Science Applications, Inc.
101 Continental Boulevard
Suite 310
El Segundo, CA 90245

1    Commander
US Army Development & Employment
     Agency
ATTN: MCDE-TED-SAB
Fort Lewis, WA 98433

1    S-CUBED
PO Box 1620
ATTN: Dr. R. Sedgwick
La Jolla, CA 92038-1620

# DISTRIBUTION LIST

| Copies | Organization | Copies | Organization |
|---|---|---|---|
| 2 | TRW<br>One Space Park, R1/2120<br>ATTN: D. Ausherman<br>M. Bronstein<br>Redondo Beach, CA 90278 | 4 | SRI International<br>333 Ravenswood Avenue<br>ATTN: Dr. L. Seaman<br>Dr. L. Curran<br>Dr. D. Shockey<br>Dr. A. L. Florence<br>Menlo Park, CA 94025 |
| 1 | United Technologies<br>Research Center<br>438 Weir Street<br>ATTN: P. R. Fitzpatrick<br>Glastonbury, CT 06033 | 2 | University of Arizona<br>Civil Engineering Department<br>ATTN: Dr. D. A. DaDeppo<br>Dr. R. Richard<br>Tucson, AZ 85721 |
| 1 | US Steel Corporation<br>Research Center<br>125 Jamison Center<br>Monroeville, PA 15146 | | University of Arizona<br>School of Engineering<br>ATTN: Dean R. Gallagher<br>Tucson, AZ 85721 |
| 1 | VPI & SU<br>106C Norris Hall<br>ATTN: Dr. M. P. Kamat<br>Blacksburg, VA 24061 | 1 | University of California<br>Los Angeles<br>ATTN: Dr. N. Ziv<br>Los Angeles, CA 90024 |
| 2 | Vought Corporation<br>PO Box 225907<br>ATTN: Dr. G. Hough<br>Dr. Paul M. Kenner<br>Dallas, TX 75265 | 1 | University of California<br>Department of Physics<br>ATTN: Dr. Harold Lewis<br>Santa Barbara, CA 93106 |
| 1 | Westinghouse, Inc.<br>PO Box 79<br>ATTN: J. Y. Fan<br>W. Mifflin, PA 15122 | 2 | University of California<br>College of Engineering<br>ATTN: Prof. W. Goldsmith<br>Dr. A. G. Evans<br>Berkeley, CA 94720 |
| 1 | Drexel University<br>Department of Mechanical Engr.<br>ATTN: Dr. P. C. Chou<br>32d and Chestnut Streets<br>Philadelphia, PA 19104 | 2 | University of Delaware<br>Department of Mechanical<br>Engineering<br>ATTN: Prof. J. Vinson<br>Prof. B. Pipes<br>Newark, DE 19711 |
| | Southwest Research Institute<br>Dept. of Mechanical Sciences<br>ATTN: Dr. U. Lindholm<br>Dr. W. Baker<br>Dr. R. White<br>Dr. M. F. Kanninen<br>Dr. C. Anderson<br>8500 Culebra Road<br>San Antonio, TX 78228 | 1 | University of Denver<br>Denver Research Institute<br>ATTN: Mr. R. F. Recht<br>2390 S. University Blvd.<br>Denver, CO 80210 |

DISTRIBUTION LIST

Copies     Organization

2     University of Florida
      Department of Engineering
        Sciences
      ATTN:  Dr. R. L. Sierakowski
             Dr. L. E. Malvern
      Gainesville, FL  32601

1     University of Oklahoma
      School of Aerospace,
        Mechanical and Nuclear
        Engineering
      ATTN:  Dr. C. W. Bert
      Norman, OK  73069

Aberdeen Proving Ground

   Dir, USAMSAA
    ATTN:  AMXSY-D
           AMXSY-MP, H. Cohen
   Cdr, USATECOM
    ATTN:  AMSTE-TO-F
   Cdr, USACSTA
    ATTN:  Mr. W. Pless
           Mr. S. Keithley
   Cdr, CRDC, AMCCOM
    ATTN:  SMCCR-RSP-A
           SMCCR-MU
           SMCCR-SPS-IL

# USER EVALUATION SHEET/CHANGE OF ADDRESS

This Laboratory undertakes a continuing effort to improve the quality of the reports it publishes. Your comments/answers to the items/questions below will aid us in our efforts.

1. BRL Report Number_____Date of Report_____

2. Date Report Received_____

3. Does this report satisfy a need? (Comment on purpose, related project, or other area of interest for which the report will be used.)_____

_____

_____

4. How specifically, is the report being used? (Information source, design data, procedure, source of ideas, etc.)_____

_____

_____

5. Has the information in this report led to any quantitative savings as far as man-hours or dollars saved, operating costs avoided or efficiencies achieved, etc? If so, please elaborate._____

_____

_____

6. General Comments. What do you think should be changed to improve future reports? (Indicate changes to organization, technical content, format, etc.)

_____

_____

_____

| | Name_____ |
| --- | --- |
| **CURRENT ADDRESS** | Organization_____ |
| | Address_____ |
| | City, State, Zip_____ |

7. If indicating a Change of Address or Address Correction, please provide the New or Correct Address in Block 6 above and the Old or Incorrect address below.

| | Name_____ |
| --- | --- |
| **OLD ADDRESS** | Organization_____ |
| | Address_____ |
| | City, State, Zip_____ |

(Remove this sheet along the perforation, fold as indicated, staple or tape closed, and mail.)